



SAPIENZA  
University of Rome

PhD SCHOOL IN  
CELL BIOLOGY AND DEVELOPMENT

XXX Cycle  
(2016/2017)

Molecular characterization of glioblastoma stem cell contribution to  
tumor vascularization and anti-angiogenic therapy resistance

PhD Student  
Mariachiara Buccarelli

Tutor  
Prof. Ada Maria Tata

Supervisor  
Dr. Lucia Ricci-Vitiani

Coordinators  
Prof. Rosa Sorrentino  
Prof. Giulia De Lorenzo

<b>ABSTRACT .....</b>	<b>4</b>
<b>INTRODUCTION .....</b>	<b>6</b>
<b>1. Glioblastoma Multiforme .....</b>	<b>6</b>
1.1 Classification and clinical aspects .....	6
1.2 Molecular and genomic alterations.....	7
1.3 Cancer stem cells and GBM .....	8
1.4 GBM, GSCs and therapy response .....	12
<b>2. Angiogenesis and cancer .....</b>	<b>14</b>
2.1 Tumor vascularization.....	14
2.2 GBM-associated neovascularization mechanisms .....	15
2.3 GSC contribution to tumor vascularization .....	18
2.4 Anti-angiogenic therapy.....	20
2.5 Resistance to anti-angiogenic therapy in GBM.....	21
<b>AIM.....</b>	<b>25</b>
<b>RESULTS .....</b>	<b>27</b>
<b>1. Molecular characterization of GdECs identifies oxidative stress pathway as a potential target for tumor endothelial cells.....</b>	<b>27</b>
1.1 Endothelial marker expression and morphological features of GSCs after trans-differentiation.....	27
1.2 In vivo evaluation of CD34 <sup>+</sup> GdEC subpopulation .....	30
1.3 MiRNA profiling of GdECs .....	31
1.4 Drug screening on GdECs .....	34
<b>2. Characterization of microvesicles indicates radiation impact on GBM microenvironment.....</b>	<b>37</b>
2.1 Quantitative analysis of HMVEC-derived MVs after radiation.....	37
2.2 Quantitative analysis of GSC-derived MVs after radiation .....	38
2.3 RNA-Seq analysis on MV content .....	39

<b>3. Molecular characterization of bevacizumab-induced infiltrative shift identifies the molecular players of tumor escape to anti-angiogenic therapy .....</b>	<b>43</b>
3.1 Effects of bevacizumab on human GBM .....	43
3.2 Effects of bevacizumab on the invasive behavior of U87MG cells in vitro .....	46
3.3 Effects of bevacizumab on U87MG brain xenografts .....	48
3.4 Bevacizumab-induced in vivo molecular changes in U87MG .....	50
3.5 Effects of bevacizumab on GSC brain xenografts.....	55
3.6 Bevacizumab-induced in vivo molecular changes in GSCs .....	56
<b>DISCUSSION.....</b>	<b>59</b>
<b>MATERIALS AND METHODS.....</b>	<b>64</b>
<b>REFERENCES .....</b>	<b>76</b>

## ABSTRACT

**Background:** Glioblastoma multiforme (GBM) is the most common and lethal primary malignant brain tumor in adults. Angiogenesis is fundamental in GBM growth and progression. GBM can adopt different strategies to build up its vasculature. Moreover, the contribution of Glioblastoma Stem-like Cells (GSCs) to GBM-associated neovascularization have important implication in GBM angiogenesis. Targeting tumor vasculature has gained more and more attention as anti-cancer therapy and many strategies have been devised to inhibit angiogenesis in GBM as well. However, recent findings indicate that the effects of anti-angiogenic treatments are transient and that tumors become refractory and more aggressive.

**Hypothesis:** GSCs directly contribute to tumor vasculature through trans-differentiation into functional endothelial-like cells. In addition, GSCs are able to participate to different processes within the vascular niche, emerging as potential escape mechanisms to counteract anti-angiogenic therapy. Among them, microvesicle-mediated intercellular communication represents a potent tool for tumor cells to influence the microenvironment promoting tumor growth and vascularization. In the vascular niche of irradiated brain, a symbiotic relationship might be hypothesized: GSCs allow the endothelial cells (ECs) to escape from radiation-induced senescence and the ECs provide differentiation cues to the tumor cells, driving its contribution to the angiogenic process. Both trans-differentiation and microvesicles trafficking might contribute to the infiltrative shift observed after bevacizumab treatment, together with other mechanisms not yet completely characterized. The investigation of this process at a molecular level could provide useful information concerning novel potential targets for alternative anti-angiogenic therapies.

**Aims:** The purpose of this project is the study of GSC contribution to tumor angiogenesis and resistance to anti-angiogenic therapy, through an integrated strategy: molecular characterization of GSC-derived endothelial cells (GdECs); investigation of the role of MVs within the vascular niche, and in particular in the crosstalk between GSCs and ECs; study of the mechanisms underlying development of bevacizumab resistance.

**Results:** Molecular characterization of GSC-derived endothelial cells (GdECs) *in vitro*, in association with a drug screening performed on these tumor cells demonstrated that GdECs are characterized by strong survival signals that confer resistance to targeted inhibition. However, we identified the oxidative stress inducer Elesclomol as the most successful antiproliferative agent on GdEC survival, suggesting that targeting the oxidative stress pathway may represent an effective strategy.

Study of the microvesicle-mediated crosstalk between GSCs and endothelial cells as emergent escape mechanism, revealed that radiation affects MV release, suggesting that it may induce modification of MV content as well.

Investigation at molecular level of the bevacizumab-induced infiltrative shift revealed that tumor cells acquire a stem-like phenotype and vascular-like behaviors after treatment. In this process, PLXDC1/TEM-7 plays an important role as responsible of perivascular spreading induced by bevacizumab.

**Conclusions:** The molecular characterization of the different mechanisms of GSC contribution to tumor vascularization provides useful insights into the development of alternative anti-angiogenic therapeutic strategy in GBM.

## INTRODUCTION

### 1. Glioblastoma Multiforme

#### *1.1 Classification and clinical aspects*

Gliomas are the most common primary malignant brain tumors in adults. About 5-6 cases out of 100,000 people are diagnosed with primary malignant brain tumors per year and 80% of them are malignant gliomas (MGs) [1-3]. They can occur anywhere in the central nervous system but primarily in the brain, in the glial tissue [4], and include astrocytomas, oligodendrogiomas, ependymomas and glioblastoma multiforme (GBM). The World Health Organization (WHO) subcategorized MGs into grades I-IV based on malignant behavior. GBM (WHO grade IV glioma) is the most lethal and common glioma subtype in adults, representing more than half of MG cases [5]. Moreover, some of lower WHO grade MGs can recur, progress, or transform into GBM, being termed secondary GBMs (over 10% of diagnosed GBM cases). The remaining 90% of diagnosed GBM cases are primary GBMs, also known as *de novo* GBM tumors [6, 7]. Primary and secondary GBMs have a similar morphology, despite the different molecular pathways underlying their developments [7, 8]. Gold-standard treatment of GBM includes maximal surgical resection followed by concurrent radiation and chemotherapy with temozolomide (TMZ, an orally available alkylating agent). Unfortunately, the tumor spreads rapidly and returns after treatment, resulting in a very poor outcome associated with a bad prognosis. GBM is still an incurable malignancy, with a median survival of about 18 months. Only about 30% of patients achieve 2-year survival and fewer than 10% survive more than 3 years. Exceptionally, a small number of patients can survive for a longer period [6, 9-13].

---

## 1.2 Molecular and genomic alterations

The many different genetic and molecular alterations present in GBM lead to modifications of several important signaling pathways that result in brain tumor growth and progression [14, 15]. Among others, the most relevant signaling pathways involved in gliomagenesis are the Epidermal Growth Factor Receptor (EGFR), the Phosphatidylinositol 3-kinase (PI3K)/Phosphatase and tensin homolog (PTEN)/AKT and the TP53/mouse double minute-2 (MDM2) pathways (Fig. 1).

EGFR is a member of the protein kinase superfamily and plays an important role in tumor progression, invasion and angiogenesis. The *EGFR* gene (7p11.2) amplification has been found in up to 60% of all GBMs and is accompanied by *EGFR* overexpression. About 68% of *EGFR* mutants present a deletion of 267 amino acids in the extracellular domain, resulting in the most common *EGFR* variant in GBM, the *EGFRvIII*, which has been associated with a poor prognosis [9].

*PTEN* is a tumor suppressor gene that negatively regulates PI3K and the levels of activated AKT in glioma cells. Its function is frequently lost in GBM patients as a consequence of loss of heterozygosity (LOH) at the 10q23.3 *locus* or gene mutations, which occur in between 15% to 40% of all GBM cases [16] and are correlated with shorter overall survival [9].

TP53 is a tumour suppressor protein encoded by the *TP53* gene at chromosome 17p13.1, and plays a role in cell cycle, cellular response to DNA damage, cell death and differentiation. MDM2 is an oncogenic protein able to negatively regulate TP53 by promoting its degradation. The TP53 signaling pathway is disrupted in GBM due to *TP53* missense mutation and/or amplification, or overexpression of *MDM2*. Mutant TP53, contrary to the wild type, is resistant to MDM2 inhibition, leading to the accumulation of mutant TP53 in tumor cells; moreover, amplification of *MDM2* gene causes the

abrogation of TP53 activity, potentially leading to uncontrolled cell proliferation and tumor formation [17].

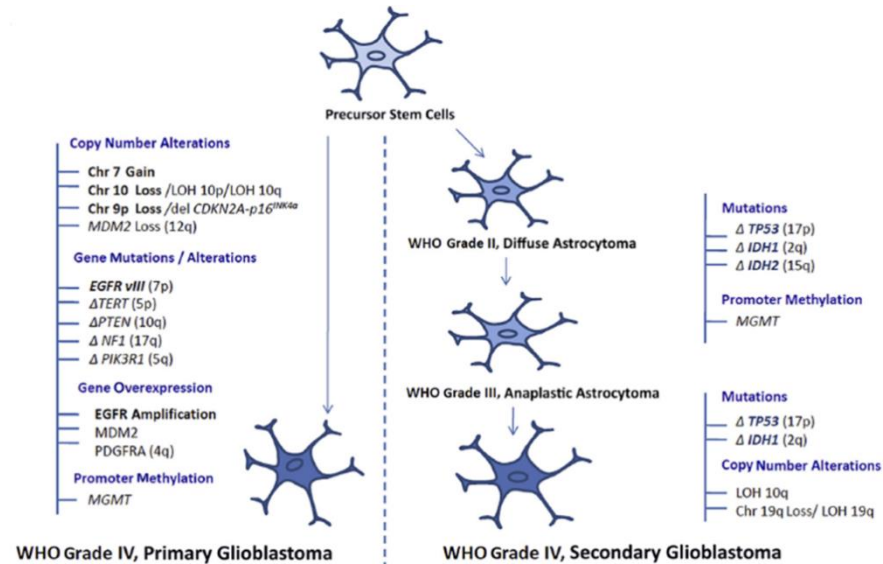


**Figure 1.** Most relevant genetic and molecular alterations in primary and secondary GBM (from [17]).

### 1.3 Cancer stem cells and GBM

Tumors are complex systems that recapitulate the complexity of organs or tissues with dynamic regulation and constituent cellular populations during tumor initiation, maintenance and progression [18]. The brain, like other organs with clearly defined cellular hierarchies in development and homeostasis, gives rise to tumors with defined cellular hierarchies, suggesting that cancer replicates ontogeny [19]. At the apex of cellular hierarchies are stem cells, that generate transient amplifying cells, which in turn create lineage-restricted progeny that are eventually fated to become the terminally differentiated effector cells. According to the original hierarchic

Cancer Stem Cell (CSC) model, malignancy was considered as a hierarchically organized tissue in which CSC population, the only responsible of the long-term progression of the tumor, generates the more differentiated bulk of tumor cells [19], which have lost their clonogenic capacity (Fig. 2A). This model relies on the idea that the CSC population is stable over time, and that CSC features are intrinsic qualities that cannot be acquired by differentiated tumor cells. However, novel data suggest that CSC phenotype is much more fluid and strongly regulated by tumor environment: this concept is defined as the dynamic CSC model (Fig. 2B). According to this emerging model, CSCs differentiate and give rise to the differentiated cell population within the tumor, but this population can dedifferentiate upon signals originating from the microenvironment [20]. The notion that CSC fate is intimately linked with the microenvironment is substantiated by several reports that suggest the presence of a CSC niche in various tumor types, by showing a close association between CSCs and a specific subset of stromal cells [21-23]. This model supports also the idea of the tumor as a highly heterogeneous tissue and the tumor cells as different in terms of long-term replication and tumorigenicity.

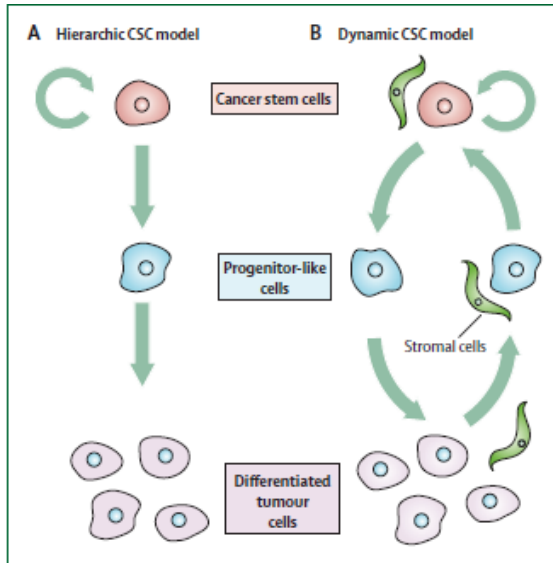


**Figure 2.** Schematic representation of hierachic (A) and dynamic (B) CSC model (from [20]).

Some years ago, several groups in parallel demonstrated that gliomas and other primary brain tumors contain self-renewing, tumorigenic cells [24-28]. Glioblastoma Stem-like Cells (GSCs) are defined as a population of cells within the tumor with the ability to self-renew, to originate differentiated progeny and to generate a tumor upon intracranial transplantation, that recapitulates the cellular heterogeneity of the parental tumor (Fig. 3).

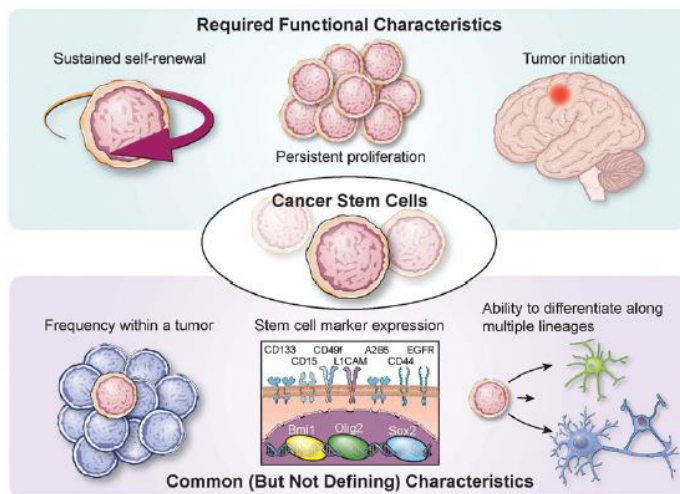


**Figure 3.** Functional criteria of cancer stem cells (*from [30]*).

During the past years, several studies have been focused on the discovery and validation of GSC enrichment methods. Most GSC markers have been appropriated from neural stem and progenitor cells (NSPCs), but the linkage between NSPCs and GSCs remains controversial. The first isolation of human NSPCs was performed using CD133 (Prominin-1) [29], a cell surface glycoprotein which was used as the first proposed marker enriches for cells with higher rate of self-renewal and proliferation and increased differentiation ability [26]. Actually, it is likely that no marker will ever be uniformly informative for CSCs, because most tissue types contain multiple populations of stem cells expressing different markers [30]. Several methods other than marker expression have been used to enrich for GSCs, such as the abilities to grow as neurospheres in serum-free medium or efflux fluorescent dyes [31, 32], but functional validation is essential to determine that the enriched cells exhibit the gold standard for CSC validation, that is the ability to recapitulate the complexity of the original patient tumor when transplanted orthotopically.

### ***1.4 GBM, GSCs and therapy response***

GBM is still an incurable malignancy mainly because of its genomic and cellular heterogeneity, high proliferative activity with infiltration into the surrounding tissues and resistance to therapy. Conventional treatment for GBM leads to an initial transient reduction/elimination of the tumor but is almost always followed by tumor recurrence, possibly with an increase in the percentage of CSCs [33], as this subpopulation of cancer cells is involved in recurrence and therapeutic resistance [34, 35]. It has been demonstrated that GSCs possess a more efficient DNA damage response machinery compared to non-stem tumor cells [34]. Moreover, it is proven that GSCs express much larger quantities of the ATP-binding cassette (ABC) transporter channels than differentiated tumor cells [36], indicating the ability to eliminate chemotherapeutic compounds more efficiently. In terms of molecular heterogeneity, different subtypes of GBM with distinct molecular profiles coexist within the same tumor and likely exhibit differential therapeutic responses [37]. A recent single-cell RNA sequencing analysis of primary GBM patients showed that cells from the same tumor have differential expression of genes involved in oncogenic signaling, proliferation, immune response and hypoxia. Furthermore, increased tumor heterogeneity was associated with decreased patient survival [38]. As regarding CSCs, although they might have the same genetic background as the bulk tumor, they can have a highly different response to therapeutic interventions according to their degree of differentiation [39].

CSCs can adopt and develop multiple mechanisms of resistance; therefore, it is necessary to consider alternative therapeutic strategies that are able to target this subpopulation of cells, including all of the intrinsic and extrinsic factors that contribute to their tumorigenic potential. Computational simulations performed on CSC-driven

malignancies exposed to drugs that selectively kill the more differentiated cells resulted in relapsing tumors, that show more invasive behavior, enrichment of CSCs and increased heterogeneity [40, 41]. Long-term clonogenicity due to the self-renewal capacity of stem-like cells is the crucial hallmark to be targeted by effective therapy, since it is associated with the most important clinical features, such as expansion and progression of the malignancy and formation of distant metastasis. Therapeutic failure and recurrence also ultimately depend on expansion of cells with self-renewal capacity. Therefore, direct assessment of clonogenicity provides a promising readout in therapeutic intervention [20]. On this matter, in a study of GBM patients it has been demonstrated that high *in vitro* clonogenicity is related to poor clinical prognosis [42]. Furthermore, recently it has been shown that the sensitivity of patient-derived GSCs to radiation and, particularly, to TMZ is linked with patients' survival [43], revealing the clinical relevance of GSC research for GBM treatment. However, the potential for non-CSCs to reacquire CSC features means that differentiated cells also need to be targeted (Fig. 4).

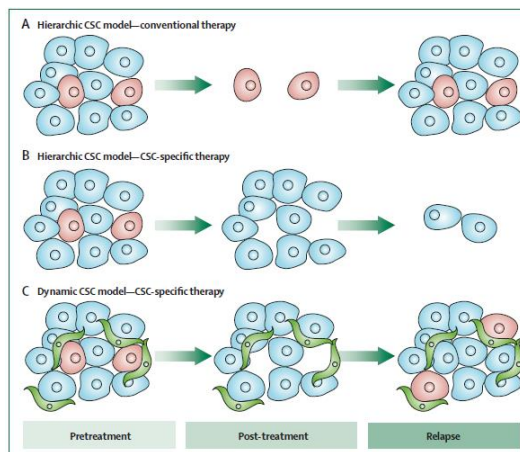


**Figure 4.** Therapy resistance in the CSC model (blue, differentiated cells; red, cancer stem cells; green, stromal cells) (from [20]).

## 2. Angiogenesis and cancer

The formation of new blood vessels is essential for tissue growth and organogenesis during development, and several mechanisms contribute to this process. Vasculogenesis, which is predominant during organogenesis and fetal development, is the formation of new blood vessels from migrating endothelial progenitor cells (EPCs), usually recruited from the bone marrow [44] and/or resident in vascular walls. Angiogenesis, common in wound healing, is the formation of novel blood vessels from pre-existing ones and involves endothelial cell (EC) proliferation with consequent sprouting and expansion of the existing vascular network [45]. Intussusception is the formation of multiple vessels from the reorganization of pre-existing vessels [46]. The normal vasculature is usually quiescent with only 0.01% endothelial cells dividing, because of the balance between pro- and anti-angiogenic factors, such as vascular endothelial growth factor (VEGF) and thrombospondin (TSP-1), respectively [47].

### 2.1 Tumor vascularization

The first description of a link between human tumors and their blood supply occurred more than 100 years ago [48]. During the following years, it has been demonstrated that tumor angiogenesis is mediated by diffusible factors produced by tumor cells [49, 50] and that if a tumor is deprived from generating its own blood supply it would not grow more than 1-2 mm in size or it might die [51].

In contrast to normal blood vessels, the tumor vasculature, particularly in GBM, is highly proliferative resulting in abnormal vessel structures. Morphologically, tumor vessels are tortuous, exhibiting dead ends leading to hypoxic regions [47]. In GBM, tumor vessels have significantly larger diameters and thicker basement membranes than those of the normal brain. These morphological

abnormalities are diagnostic features in brain tumors, especially GBMs. Aberrant microvasculature typically appears as “glomeruloid tufts”, consisting of multilayered, mitotically active ECs and perivascular cells [52, 53].

The initiation of angiogenesis in tumors is thought to be activated by the resulting hypoxia due to the high density of tumor cells. Hypoxia stimulates the expression of the transcription factor hypoxia inducible factor-1  $\alpha$  (HIF-1 $\alpha$ ), which triggers the production of VEGF, among other pro-angiogenic growth factors [54]. Thus, the tumor vasculature is responsive to the microenvironment. The shift toward the pro-angiogenic factors determines the so-called “angiogenic switch”, the passage from the pre-angiogenic to the angiogenic phenotype of the tumor. This will cause activation of ECs in local blood vessels, resulting in basement membrane and extracellular matrix (ECM) degradation, EC migration and proliferation and tube formation to form new vascular sprouts [55], and the onset of the tumor angiogenesis process. Tumor ECs overexpress VEGF receptors, therefore an environment of high VEGF will cause increased endothelial cell proliferation, migration and blood vessel permeability [52].

## ***2.2 GBM-associated neovascularization mechanisms***

In addition to the mechanisms occurring in normal vasculature, several other mechanisms unique to tumor vascularization have been identified. For historical reasons, the term “angiogenesis” is used to describe all of these methods of blood vessel recruitment by tumors (Fig. 5).

Temporally, vascular co-option is the first mechanism by which gliomas achieve their vasculature. This process involves organization of tumor cells into cuffs around normal microvessels [56], thus the existing vasculature is co-opted by cancer cells. This mechanism was first described by Holash et al using a rat glioma model, and co-opted

vessels were characterized for the expression of angiopoietin-2 (ANG-2) [57, 58]. Vessel co-option is independent of the classic angiogenic switch and occurs in the absence of angiogenic growth factors [55].

In tumor models, it has been shown that vascular co-option precedes angiogenesis by up to 4 weeks [56]. Then, tumor cells exploit the existing vessels to build up their own vascular network. Angiogenesis was described in GBM in 1976 by Brem in rabbit corneas transplanted with GBMs, suggesting an *in vivo* production of a “vasoformative substance” [59]. The result of the neoplastic angiogenic process is a characteristically abnormal vascular network, with abnormal branching and perfusion. GBMs in particular have immature vasculature, with excessive leakiness that can contribute to the breakdown of the blood-brain barrier (BBB) [56], a structure composed of endothelial cells, pericytes and astrocytes, that selectively restricts the exchange of molecules between the intracerebral and extracerebral circulatory systems.

Blood vessels can also develop by another mechanism of tumor neovascularization, that is adult vasculogenesis. Bone marrow endothelial progenitor cells can enter blood circulation with direct incorporation into functional vasculature (reviewed by [52]). Tumor cells, particularly glioma cells, produce stromal cell-derived factor-1 (SDF-1) causing the migration of endothelial cells to the tumor site. This mechanism is especially important during recurrent disease to allow tumor cells to continue to grow after radiation-induced damage to the vasculature [60].

A fourth mechanism of glioma vascularization is vascular mimicry. This process is defined as the ability of highly invasive and genetically dysregulated tumor cells to form functional vessel-like structures, getting incorporated into the blood vessel wall. It was first

described in uveal melanoma as the formation of a circulatory system by dedifferentiating tumor cells [61]. Evidence for vascular mimicry in gliomas has also been published (reviewed by [56]), suggesting a link between vascular mimicry in GBMs and vascular radioresistance and a correlation with WHO tumor grade.

The most recently described mechanism of glioma neovascularization is the trans-differentiation of GSCs into ECs, including both a phenotypic change and the expression of typical endothelial-specific markers. As with vascular mimicry, this hypothesis originated with human cutaneous melanoma models. In 2010, two groups independently reported the trans-differentiation of GSCs into ECs *in vitro* [62, 63], showing that a proportion of vascular cells within human GBM contained genetic alterations typically reported in GBM cells and not seen in vascular endothelial cells (such as *EGFR* amplification). In GBM, as much as 60% of the endothelial cells express the same somatic mutations as the parent tumor, suggesting a neoplastic origin of the tumor vasculature which means that a significant portion of the tumor vasculature is derived from GBM cells [63]. Moreover, it has been also demonstrated that GSCs are able to trans-differentiate into pericytes [64].

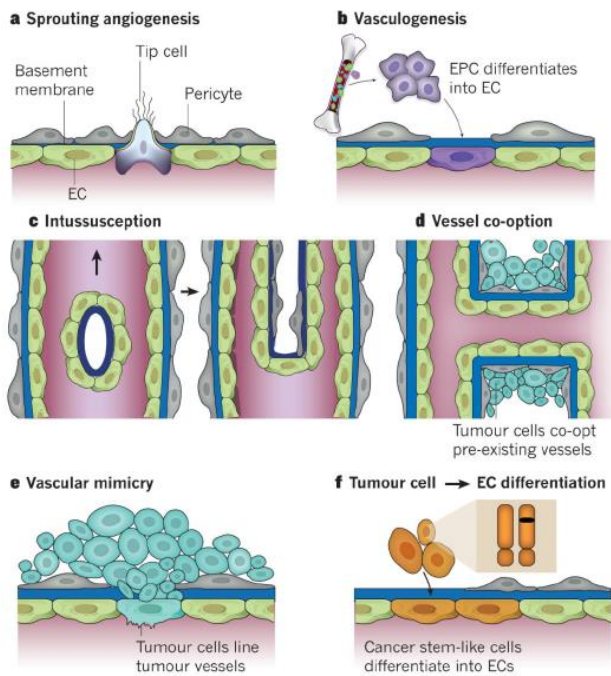


**Figure 5.** Modes of blood vessel formation in normal tissues (a-c) and tumors (d-f) (from [81])

### 2.3 GSC contribution to tumor vascularization

As mentioned above, recently it has become increasingly clear that GSCs play an important role in the process of tumor angiogenesis. Several studies demonstrated the contribution of GSCs to the different but interlinked mechanisms of glioma neovascularization. The plasticity of GSCs may contribute to vascular mimicry: it has been proposed that this process could represent an incomplete trans-differentiation of GSCs toward an endothelial phenotype [62]. Indeed, overlap is evident from recent reports of both vascular

mimicry and trans-differentiation, suggesting that these mechanisms are intimately connected [56].

GSCs can also exert paracrine effects on ECs by secretion of soluble factors to stimulate tumor angiogenesis. *In vitro* studies revealed that conditioned medium from GSC-enriched cell population contains approximately 10-20 fold higher levels of VEGF than medium from non-GSC-enriched cell population, promoting human microvascular endothelial cell migration and tube formation [65]. In addition to VEGF, GSCs also produce other pro-angiogenic growth factors such as SDF-1, which mediate the recruitment of EPCs contributing to the vasculogenesis process [66].

Endothelial cells have also been shown to secrete factors that maintain GSC self-renewal and survival through activation of the mammalian target of rapamycin (mTOR) signaling pathway [67]. Conditioned medium from ECs can rescue GSCs from apoptosis and autophagy induced by growth factor deprivation [68]. In the past years, several studies focused on the identification of the signaling pathways involved in the interaction between GSCs and ECs. A study on human GBM tissues demonstrated that GSCs are close to CD34<sup>+</sup> endothelial cells, suggesting the presence of a vascular niche which regulates GSC self-renewal and tumorigenicity [23]. On the other hand, the distribution of tumor-derived ECs does not appear to be homogeneous throughout the tumor. These ECs were found more frequently in the core of the tumor as compared to the periphery [69]. This correlates with the high density of GSCs found in the hypoxic core of the tumor than in the periphery [70]. An emerging mechanism of interaction between GSCs and ECs within the vascular niche is represented by microvesicles (MVs), spherical vesicles of different sizes produced by several types of cells through outward budding and fission of the plasma membrane [71]. It has been reported that GBM cells release MVs as well, containing messenger

RNAs (mRNAs), micro RNAs (miRNAs) and pro-angiogenic proteins [72]. Moreover, it has been demonstrated that a direct MV transfer from GBM cells to ECs exists, and that MVs secreted by GBM cells under hypoxic conditions are able to induce microvascular sprouting *in vitro* [73].

## ***2.4 Anti-angiogenic therapy***

Since the observation of Folkman in 1971 [51] that tumor growth is dependent on angiogenesis, research in inhibition of angiogenesis as a therapeutic strategy against cancer gains more and more attention. Anti-angiogenic therapy was originally developed to “starve” primary and metastatic tumors by blocking blood vessel formation and recruitment [74]. More recent studies showed that in addition to providing oxygen and nutrients, the neovasculature can secrete growth factors (angiocrine signaling), which can stimulate growth of adjacent tumor cells directly, potentially identifying new targets for therapy [75]. Anti-angiogenic strategy was expected to be an efficient anti-cancer treatment for different reasons: the target cells are ECs in direct contact with the blood, ensuring easy delivery of therapeutic compounds; targeting only a few ECs will cause the starvation of many tumor cells depending on a single capillary. Moreover, ECs are considered to be genetically stable cells, reducing the chance of acquired drug resistance, and as ECs throughout the body are generally quiescent, anti-angiogenic therapy can be expected to have limited side effects because it targets only activated ECs [76, 77]. In addition, tumor neovascularization can be an attractive target particularly for malignant brain tumors because of the high degree of neovascularization, avoidance of problems related to crossing the blood-brain barrier and resulting normalization of

vascular networks, leading to synergism with other therapeutic strategies [56].

Besides the direct injury to blood vessels and reduced delivery of oxygen and nutrients to high metabolic tumor cells, another potential mechanism of anti-angiogenic therapy is vascular normalization. This concept, introduced by Jain [78], states that anti-angiogenic treatment merely affects the immature vasculature and leaves the mature vessels unaltered, leading to improvements in tumor vessel function, increased perfusion of the tumor and subsequent increase of oxygenation [79]. Vascular normalization is thought to interrupt the vicious circle that is driven by hypoxia and that leads to upregulation of VEGF. Therefore, a widely held conception is that anti-angiogenic treatment ‘works’ in the clinic because it improves the delivery of co-administered chemotherapy [80].

However, recent findings indicate that the effects of anti-angiogenic treatments are transient and that tumors become refractory and more aggressive.

## ***2.5 Resistance to anti-angiogenic therapy in GBM***

Resistance to anti-angiogenic therapy can be classified into intrinsic resistance, when tumors never show any response to treatment, and acquired resistance, when patients develop resistance during the course of treatment [81]. Several mechanisms have been proposed to contribute to these phenomena: heterogeneity of tumor vasculature, alternative pro-angiogenic signaling pathways, infiltrating stromal cells, adaptation of tumor cells to conditions of stress, increased alternative mechanisms of tumor vascularization (such as vascular mimicry and vessel co-option), increased tumor aggressiveness (Fig. 6). These mechanisms have also been described in gliomas after anti-

angiogenic treatment, alone or in combination with other therapeutic agents [82].

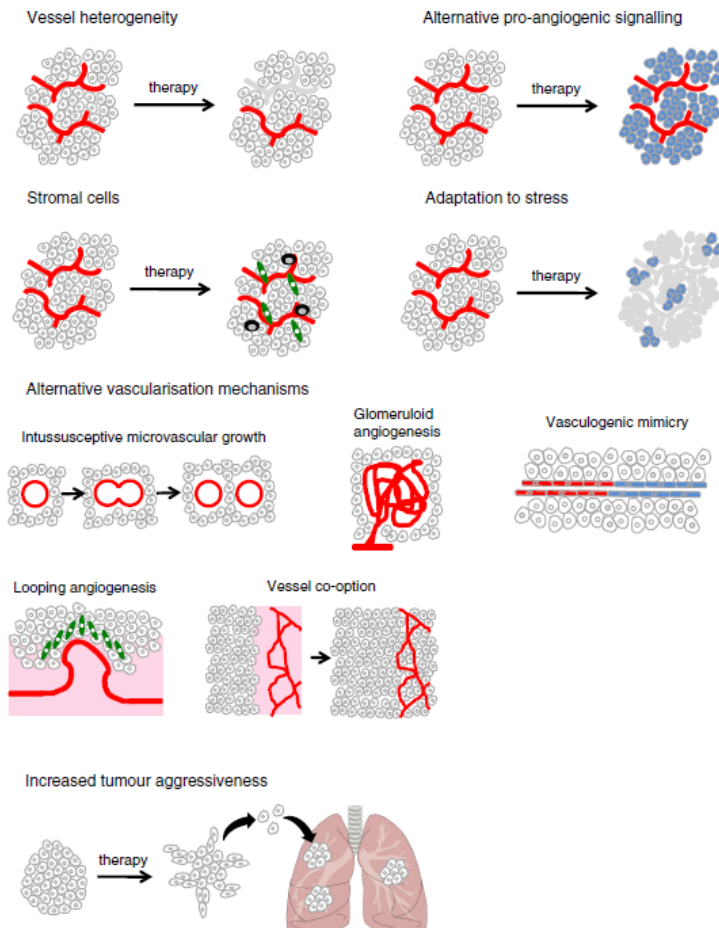


**Figure 6.** Potential mechanisms involved in resistance to VEGF-targeted therapy (from [80]).

In the past years, several approaches aimed at targeting glioma neovasculature have been proposed. Since GSCs are closely related

---

to the tumor vasculature, anti-angiogenic therapy might also represent a way to target GSCs.

GBM is characterized by the release of VEGF and high levels of this pro-angiogenic factor have been reported in plasma and tumor fluid of GBM patients. Moreover, VEGF overexpression has been correlated with prognosis in GBM [83]. Therefore, the VEGF pathway has been the target of most of the anti-angiogenic agents developed for GBM treatment as adjuvant to normalize blood vessels and control abnormal angiogenesis and tumor growth [82]. Among others, the most extensive clinical experience with anti-angiogenic therapy in GBM has been with bevacizumab (BV, Avastin<sup>®</sup>), a humanized monoclonal antibody that binds specifically to VEGF-A. In 2009, the use of bevacizumab has been approved by the US Food and Drug Administration (FDA) in the treatment of recurrent GBM [84], and it represents the only anti-angiogenic agent currently approved for use in this setting. Although for GBM recurrent patients it shows some benefit and clinical efficacy, its effectiveness is still debated. Two recently published Phase III trials on newly diagnosed GBM demonstrated no significant difference in overall survival (OS) between treated and untreated patients [85, 86]. In addition, in recurrent GBM the benefit is temporary since patients generally relapse [47], reflecting development of resistance to anti-angiogenic therapy. It has been reported that GBM adopts a more infiltrative tumor growth pattern upon treatment with VEGF-targeted therapy [87, 88], presumably due to a decrease in tumor oxygenation which has been shown to increase tumor invasion in animal models [89]. The resultant decrease in blood flow may also decrease nutrient delivery, placing additional physiologic stress, which may contribute to the phenotypic shift of the tumor becoming more invasive [87]. The so-called “infiltrative shift” described in GBM after bevacizumab treatment suggests that inhibition of angiogenesis is

even a driving force for tumor conversion to a greater malignancy, reflected in increased invasion and dissemination into surrounding tissues [82]. *In vitro* and *in vivo* studies demonstrated the higher invasive capacity of bevacizumab-resistant GSCs showing that re-treatment of bevacizumab unresponsive tumors only exacerbates tumor growth and invasion, and does not appear to diminish blood vessel growth [90]. In addition, it has been reported that bevacizumab resistance exhibits an increase in stem cells as ascertained by markers such as Sox2 and Nestin [91]. Therefore, several mechanisms can contribute to the anti-angiogenic therapy-induced invasive growth program of the tumor, enhancing alternative VEGF-independent mechanisms and/or activating alternative pro-angiogenic pathways, leading to resistance to anti-angiogenic therapy.

## AIM

The aim of this project is the study of GSC contribution to tumor angiogenesis and resistance to anti-angiogenic therapy.

According to this aim, the project has been performed using different approaches: molecular characterization of GSC-derived endothelial cells (GdECs); investigation of the role of MVs within the vascular niche, and in particular in the crosstalk between GSCs and ECs; study of the mechanisms underlying development of bevacizumab resistance.

Since the evidence that GSCs are able to trans-differentiate into ECs has emerged, several studies have been focused on investigating this new mechanism of GBM neovascularization. Furthermore, it has been reported that GdECs are non-VEGF-dependent ECs [69]. Thus, it might be hypothesized that this subpopulation of cells represents an escape mechanism to anti-angiogenic therapy, contributing to the development of resistance.

Other emergent mechanisms promoting resistance to anti-angiogenic treatment are the ability of tumor cells to shape the microenvironment and the interaction with the stromal cells. It has been reported that GBM conditioned medium prevents replicative senescence by human umbilical vein endothelial cells (HUVECs) [92], suggesting that soluble factors released by GBM cells may influence the local environment. Therefore, it might be hypothesized that MVs released by GBM cells could protect the brain endothelium by radiation-induced senescence, promoting tumor growth and vascularization. On the other hand, ECs could provide soluble factors through MVs promoting GSC trans-differentiation and contribution to the angiogenesis process.

Both the processes described above might contribute to the infiltrative shift observed after bevacizumab treatment, together with other mechanisms not yet completely characterized. The investigation of this process at a molecular level could provide useful information concerning novel potential targets for alternative anti-angiogenic therapies.

## RESULTS

### 1. Molecular characterization of GdECs identifies oxidative stress pathway as a potential target for tumor endothelial cells

#### *1.1 Endothelial marker expression and morphological features of GSCs after trans-differentiation*

As already described, one of the most important mechanisms of GSC contribution to tumor vasculature is the trans-differentiation into functional ECs. In our laboratory, during the last years we collected more than seventy patient-derived GSC lines, validated for their stem cell properties [43]. In order to characterize at a molecular level GSC trans-differentiation ability, we started to collect GdECs from our collection of GSC lines.

First of all, we tested different protocols to define the better condition for the endothelial differentiation and the most suitable markers to evaluate and select the differentiated cell population. We used 4 GSC lines (GSC#1, GSC#61, GSC#83, GSC#163) derived from different GBM patients. GSCs were cultured under normoxia or hypoxia, using the following different culture conditions: endothelial medium; stem cell medium supplemented with serum and endothelial growth factors; stem cell medium, with or without serum, as negative controls. Two weeks after, we evaluated the expression of the endothelial marker CD31 by cytofluorimetric analysis, as marker for the acquisition of an endothelial phenotype [93]. This analysis revealed that GSCs cultured under hypoxic condition in stem cell medium supplemented with serum and endothelial growth factors

show higher expression of CD31 compared to other culture conditions (Fig. 7).

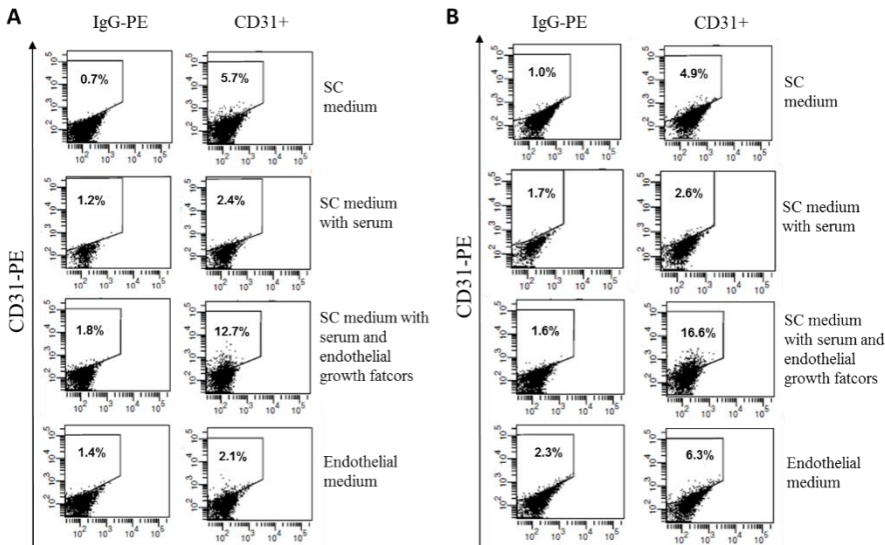


**Figure 7. A-B.** FACS analysis based on CD31 expression of a representative GSC line (GSC#83) cultured in different medium and oxygen conditions (**A**, normoxic; **B**, hypoxic).

Then, using stem cell medium supplemented with serum and endothelial growth factors we decided to evaluate also CD34 expression, which is widely regarded as a marker of vascular endothelial progenitor cells [94]. In all of the GSC lines analyzed, we observed higher percentage of CD34-expressing cells in endothelial conditions, compared to stem cell culture conditions (Fig. 8).

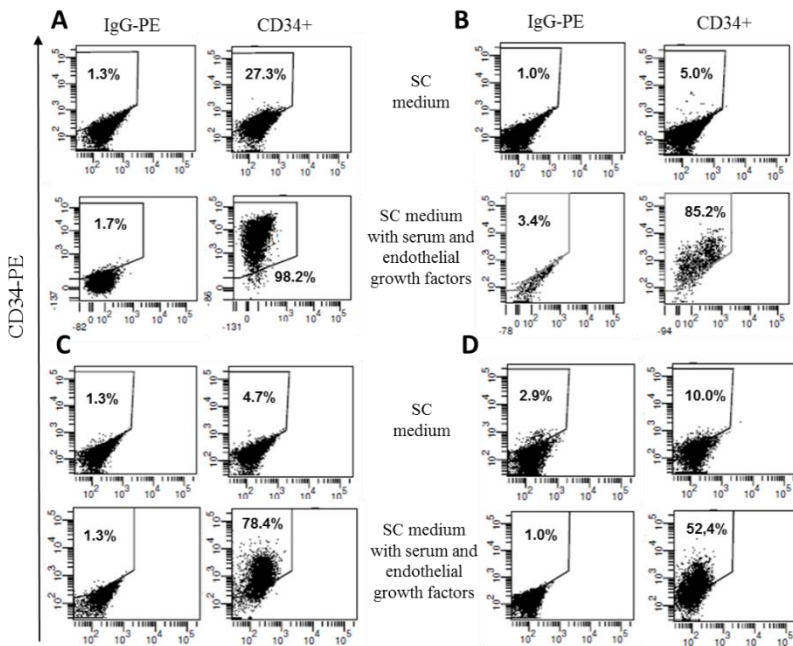


**Figure 8. A-D.** FACS analysis based on CD34 expression of the four GSC lines in stem cell (SC) medium or endothelial conditions under hypoxia. **A**, GSC#163; **B**, GSC#1; **C**, GSC#61; **D**, GSC#83.

Moreover, after two weeks under these culture conditions, GSCs underwent a morphological change from tumorspheres to continuous net-like structures (Fig. 9).

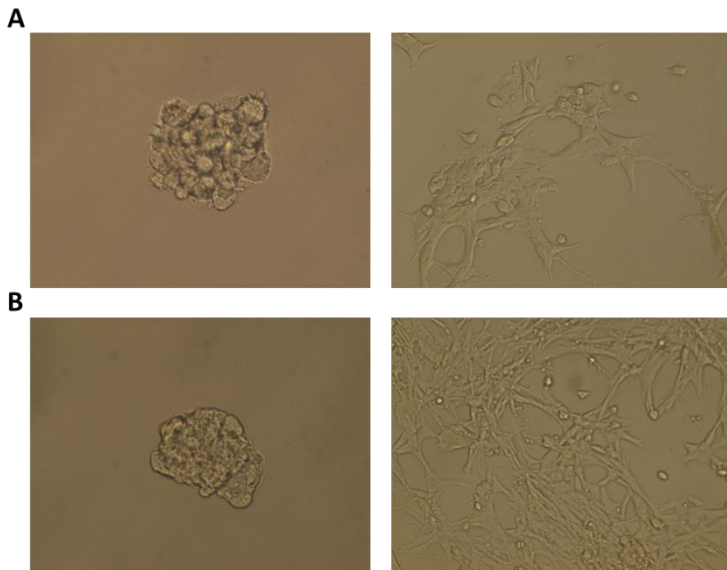


**Figure 9. A-B.** Morphological changes of two representative GSC lines (**A**, GSC#1; **B**, GSC#163) after being induced to trans-differentiate for 2 weeks. **Left panel**, tumorspheres in stem cell medium; **right panel**, net-like structures under endothelial conditions (magnification 10X).

### **1.2 In vivo evaluation of CD34<sup>+</sup> GdEC subpopulation**

To investigate the functional properties of GSCs trans-differentiated in endothelial-like cells, we decided to evaluate their tumorigenic potential through subcutaneous injection in immunodeficient mice. To this aim, using one out of the four GSC lines previously characterized (GSC#163), we performed a fluorescent-activated cell sorting (FACS) based on CD34 expression after 2 weeks in endothelial conditions, in order to obtain two subpopulations of cells with different CD34-expression levels (CD34<sup>low</sup> and CD34<sup>high</sup>). Immunohistochemical analysis of tumor brain xenografts revealed that xenografts originated from CD34<sup>low</sup> cells showed typical

features of differentiated tumors (Fig. 10A). Conversely, those generated by CD34<sup>high</sup> cells showed typical properties of a less differentiated tumor with areas of necrosis (Fig. 10B), and high percentage of proliferating cells.

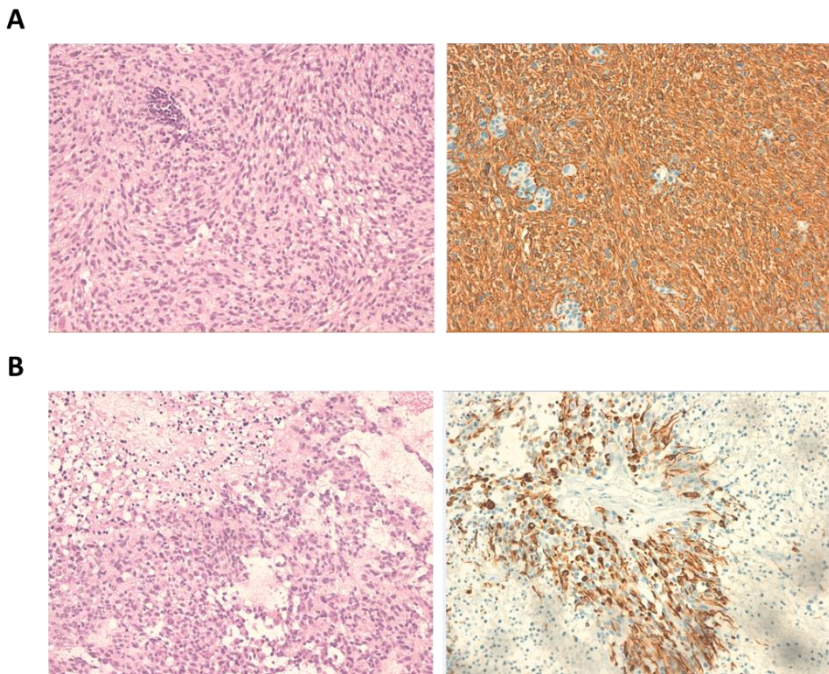


**Figure 10. A-B.** Immunohistochemical analysis of CD34<sup>low</sup> (A) and CD34<sup>high</sup> (B) GdEC subcutaneous tumor xenografts based on the expression of the astrocytic marker glial fibrillary acidic protein (GFAP, **right panels**), showing tumors with different levels of differentiation. (**Left panels**, haematoxylin and eosin staining; magnification 200X).

### 1.3 MiRNA profiling of GdECs

MiRNA expression profile analysis of a subpopulation of tumor cells can allow to dissect the molecular mechanisms underlying their maintenance, pointing out which signal transduction pathways are

involved. In order to identify signaling pathways with potential relevant functions in GdEC survival, we performed miRNA profiling of the four GSC lines either cultivated in stem cell medium or in endothelial conditions. The miRNA expression pattern was analyzed by principal component analysis (PCA, Fig. 11A). Hierarchical clustering of global miRNA expression pattern revealed two distinct clusters: the "SCs" and the "Endo" clusters. The signature underlying SCs vs Endo clustering included 21 miRNAs, whose expression is upregulated in "Endo" compared to "SCs" cluster (Fig. 11B).

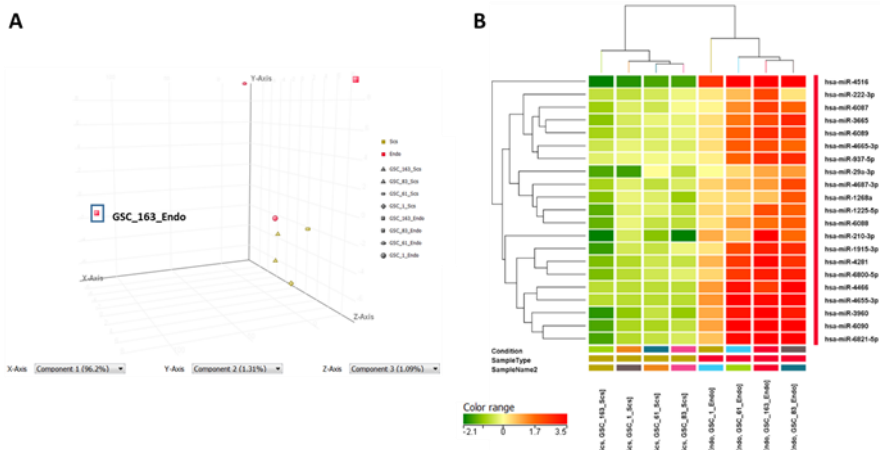


**Figure 11.** **A.** Principal Component Analysis (PCA) of miRNA expression pattern. **B.** Hierarchical clustering of global miRNA expression pattern, identifying 21 miRNAs upregulated in the “Endo” cluster.

Excluding GSC#163 pair, which resulted too different from the other samples, by combining an unpaired hierarchical clustering we identified a list of 14 miRNAs differentially expressed between the two clusters (Fig. 12A). Then, a paired hierarchical clustering revealed a signature of three miRNAs, miR-4516, miR-1281 and

miR-1825, able to clearly distinguish GSCs cultivated in stem cell medium or differentiated in endothelial conditions (Fig. 12B).

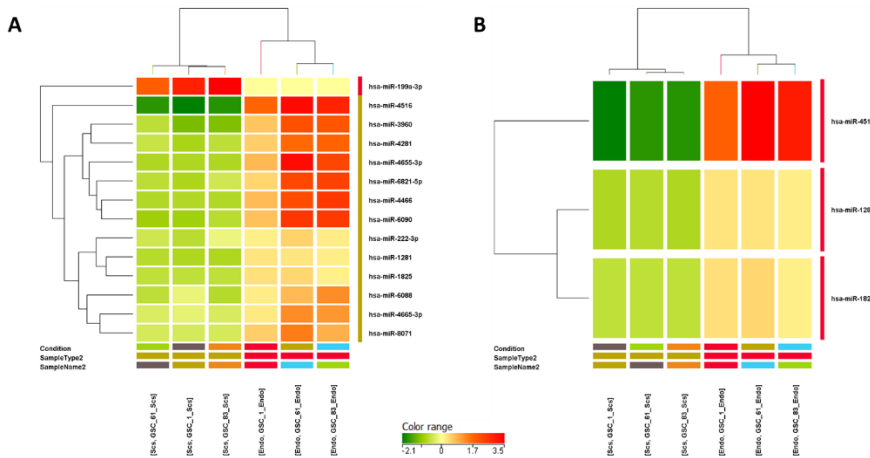


**Figure 12.** Unpaired (A) and paired (B) hierarchical clustering of global miRNA expression, identifying a signature of three miRNAs.

A Gene Set Enrichment Analysis (GSEA) of the three miRNA targets, revealed a modulation of genes associated with pathways involved in different processes such as angiogenesis, hypoxia and reactive oxygen species (ROS) metabolism (Fig. 13). These results suggest a possible implication of these three miRNAs, considered as interdependent genes, into the GSC-associated neovascularization process.

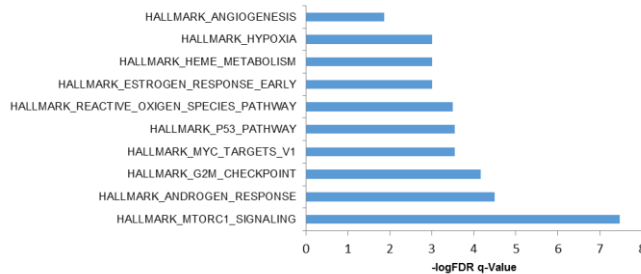


**Figure 13.** Signaling pathways associated with the genes modulated by the three miRNAs identified by GSEA analysis based on their targets.

#### 1.4 Drug screening on GdECs

GSEA revealed signaling pathways that could be important for GdEC survival and associated angiogenesis. GdECs are non-VEGF-dependent ECs [69], therefore this subpopulation of cells could play a role in the development of resistance to anti-angiogenic treatment, as alternative activated VEGF-independent mechanism of neovascularization. Selective targeting of ECs generated by GSCs in mouse xenografts resulted in tumor reduction and degeneration, indicating the functional relevance of the GSC derived endothelium [62]. Hence, GdECs might represent a novel target for alternative therapeutic strategies. For these reasons, we decided to assess the effect of a selection of compounds able to counteract most of the GdEC survival pathways, including those highlighted in GSEA analysis. A commercially available anti-cancer drug library was screened on the four selected GSC lines either cultivated in stem cell medium or differentiated in GdECs. Such a unique collection of bioactive compounds includes 349 experimental, investigational or FDA-approved kinase inhibitors targeting most cancer-related pathways (PI3K, HDAC, mTOR, MAPK, CDK, Aurora Kinase, JAK, etc.). Human dermal microvascular endothelial cells

(HMVECs) were used as a control of normal (non-tumoral) EC lines. After 72h treatment, both GSCs in stem cell condition and even more GdECs showed a lower sensitivity to most of the compounds tested than HMVECs. However, a set of chemotherapeutics as well as inhibitors of Bcl-2 family, PI3K, HDAC, mTOR and 20S proteasome, yielded a significant decrease in cell number also in GdECs (Fig. 14). Our functional data derived from *in vitro* kinase inhibition confirm the existence of strong survival signals in both GSCs and GdECs that confer resistance to targeted inhibition.

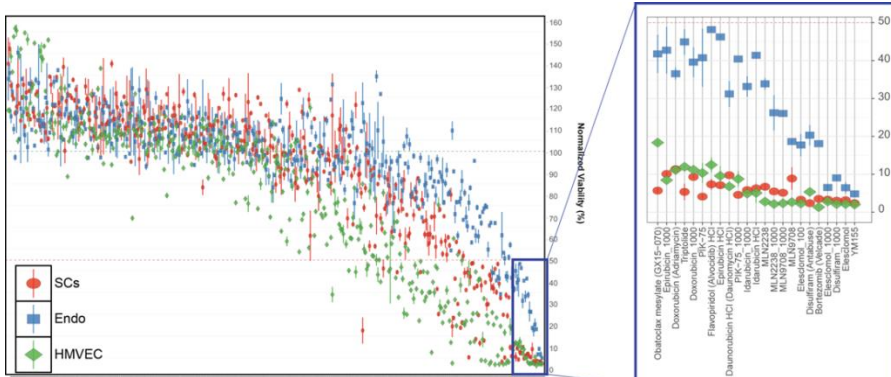


**Figure 14.** Kinase inhibitor library screening in a representative GSC line either in stem cell medium (SCs) or in endothelial conditions (Endo) and in HMVECs. Cell viability is reported as mean $\pm$ SD ( $n=3$ ) of standardized values (*z score*) for each cell line treated with the kinase inhibitor library at 1 $\mu$ M for 72h.

Since the screening was performed at a high concentration, to assess the specificity of kinase inhibitor effect and rule out off-target effects, we performed concentration-response assays. Most of the compounds were inactive at submicromolar concentrations, as shown by markedly high EC<sub>50</sub> values (half maximal effective concentration) for all cell lines. Among the agents active at submicromolar concentrations, Elesclomol (STA-4783), a potent oxidative stress inducer, was the most effective antiproliferative agent yielding a high

degree of sensitivity across both the GSCs in stem cell medium and GdEC lines. It has been shown that Elesclomol induces apoptosis in cancer cells through the induction of oxidative stress. Treatment of cancer cells *in vitro* with Elesclomol resulted in the rapid generation of ROS and the induction of a transcriptional gene profile characteristic of an oxidative stress response [95].

## 2. Characterization of microvesicles indicates radiation impact on GBM microenvironment

### 2.1 Quantitative analysis of HMVEC-derived MVs after radiation

In physiological as well as pathological processes, MVs and other extracellular vesicles (EVs) are able to deliver their contents of proteins, lipids and RNAs following interaction with recipient cells, causing possible alteration of cell phenotype. It has been reported that in tumor microenvironment various cellular insults cause cancer cells to increase the release of and alter the molecular composition of tumor EVs, including cancer therapies such as ionizing radiation [96-98]. In order to investigate MV-based intercellular communication in GBM, we decided to evaluate the effects of radiation on MVs in the tumor microenvironment, considering that GBM conditioned medium protects HUVEC by radiation-induced senescence [92].

We isolated MVs from either irradiated (10Gy and 50Gy) or sham irradiated HMVECs by ultracentrifugation. Western blot analysis showed that isolated MVs had known markers, such as tumor susceptibility gene 101 protein (tsg-101) and ALG-2-interacting-protein X (Alix) (data not shown). We were able to count secreted MVs by flow cytometry, using a fluorescent fatty acid molecule incorporated by the cells during MV-membrane biogenesis. We observed a significant increase of the number of released MVs per cell in both 10Gy- and 50Gy-irradiated cells compared to control cells (Fig. 15A), confirming an increase in MV release under stress conditions. To verify that HMVEC-derived MVs could be transferred to a recipient cell, fluorescent-labeled MVs were incubated with

GSCs and the uptake was confirmed by analyzing the cells by cytofluorimetric analysis (Fig. 15B).

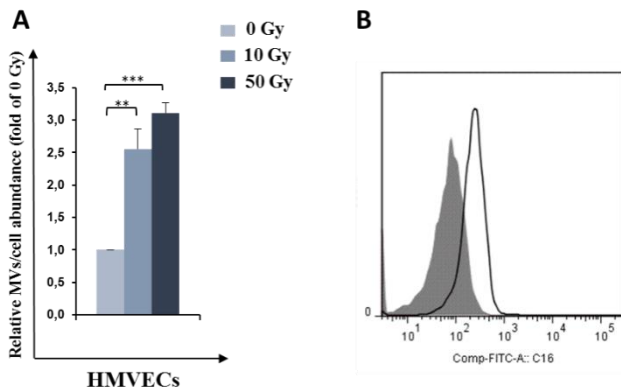


**Figure 15.** **A.** Measurement of MVs/cell abundance of irradiated HMVECs relative to sham irradiated cells. Values are mean±SD from at least three independent experiments (\*\*  $p<0.01$ ; \*\*\*  $p<0.001$ ). **B.** FACS analysis based on green fluorescence of one representative GSC line (GSC#61) after HMVEC-derived MVs uptake (*shaded histogram*=GSC control sample; *open histogram*=GSCs incubated with MVs).

## 2.2 Quantitative analysis of GSC-derived MVs after radiation

By using the same approach described for HMVECs, we isolated and validated MVs derived from four GSC lines (GSC#1, GSC#61, GSC#83, GSC#163), either irradiated (10Gy and 50Gy) or sham irradiated. As observed for HMVECs, after radiation all of the four GSC lines analyzed showed a significant increase of the number of released MVs per cell compared to non-irradiated cells (Fig. 16A). Then, fluorescent-labeled MVs derived from one representative GSC line (GSC#163) was incubated with HMVECs and the uptake was confirmed by flow cytometry (Fig. 16B).

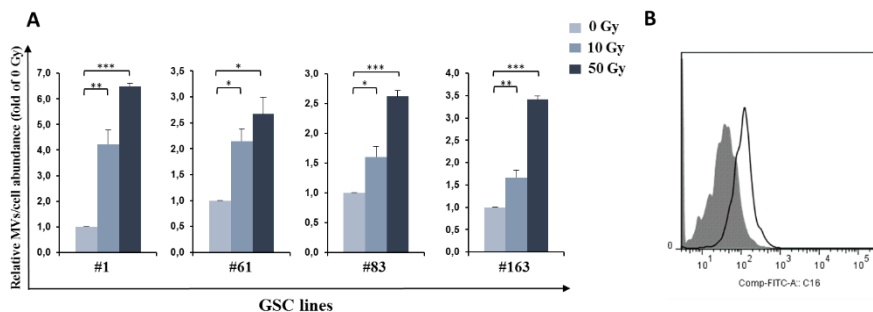


**Figure 16.** **A.** Measurement of MVs/cell abundance of irradiated GSCs relative to sham irradiated cells. Values are mean $\pm$ SD from at least three independent experiments (\*  $p<0.05$ ; \*\*  $p<0.01$ ; \*\*\*  $p<0.001$ ). **B.** FACS analysis based on green fluorescence of HMVECs after GSC-derived MVs uptake (shaded histogram=HMVEC control sample; open histogram=HMVECs incubated with MVs).

### 2.3 RNA-Seq analysis on MV content

Since it has been reported that MV mRNA and protein composition is affected by ionizing radiation [98], we decided to analyze the total RNA isolated from MVs by RNA sequencing analysis in order to identify a differential expression pattern between 50Gy irradiated-and sham irradiated-derived MVs. The analysis was performed on MVs derived from HMVECs and one out of the four GSC lines (GSC#61). The correlation analysis between samples at transcription level showed that the two cell types differ from each other more than they differ from the treatment (Fig. 17).

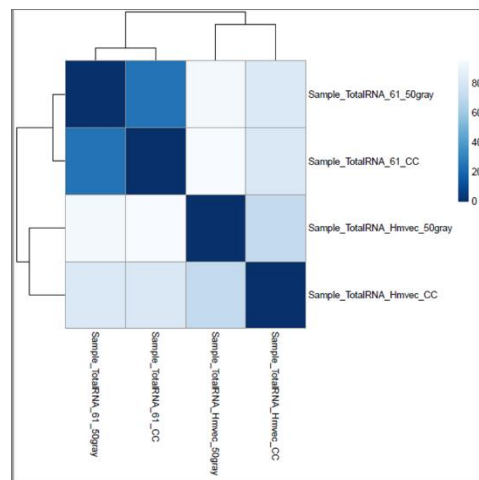


**Figure 17.** Heatmap of the transcript expression. The intensity of the color represents the distance between the samples (blue=identity; white=no similarity).

Considering the *log fold ratio* for each transcript for each cell line, an interesting observation is that HMVECs are far more sensible to the treatment, as demonstrated by the number of transcripts which expression is modulated in the irradiated-derived MVs compared to control (Fig. 18).

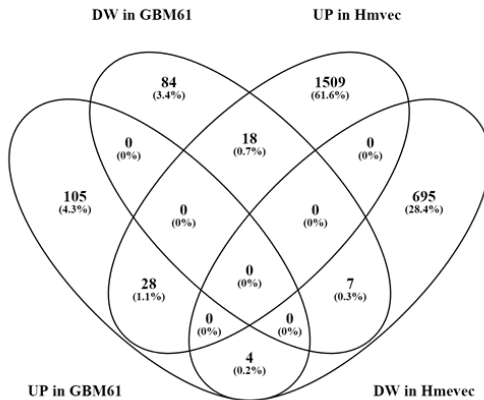


**Figure 18.** Venn diagram representation of the number of transcript changes in irradiated-derived MVs compared to sham irradiated-derived MVs. *Log fold ratio* was greater or lower than 2 or -2 for upregulated or downregulated transcripts, respectively.

Comparing the irradiated-derived MVs vs sham irradiated-derived MVs regardless of the cell line, we obtained a list of the transcripts that are modulated in both conditions (Fig.19).

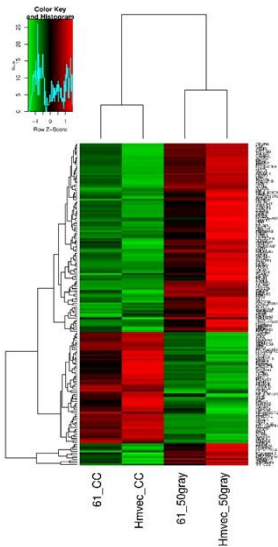


**Figure 19.** Heatmap of the differential transcript expression. The expression values of the transcripts in the MVs derived from the two cell lines were included in a statistical model comparing MVs derived from irradiated cells vs MVs derived from sham irradiated cells. The intensity of the color represents differential *z score* values (*red*=increase, *green*=decrease, in respect of the average expression in all of the samples).

### **3. Molecular characterization of bevacizumab-induced infiltrative shift identifies the molecular players of tumor escape to anti-angiogenic therapy**

#### ***3.1 Effects of bevacizumab on human GBM***

Although bevacizumab currently is the only FDA-approved targeted agent for recurrent GBM, tumor regrowth after initial response is frequently seen. Several studies describe the infiltrative growth of GBM after bevacizumab, with the acquisition of a gliomatosis-like growth pattern as consequence of a phenotypic change [99, 100]. In order to investigate the effects of bevacizumab treatment on GBM patients, a surgically resected temporal lobe was assessed by histology and fluorescence microscopy, in collaboration with the Institute of Neurosurgery at Catholic University of Rome. This GBM patient had undergone a first craniotomy for partial removal of a right parietal GBM (Fig. 20, *left*). After surgery, he received radiotherapy and TMZ according to the Stupp protocol [11]. The patient had undergone a second craniotomy after 10 months for local tumor recurrence (Fig. 20, *centre* and *right*).

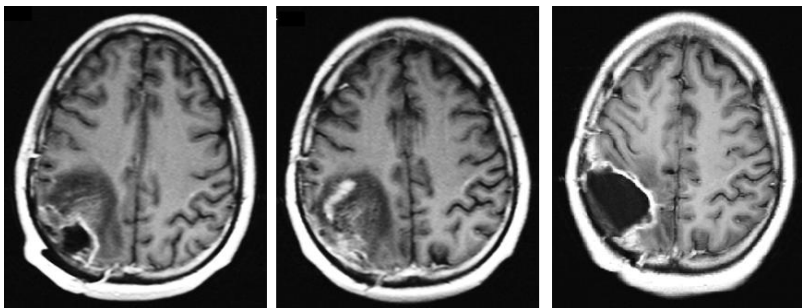


**Figure 20.** Axial gadolinium-enhanced T1-weighted MR images showing: partial removal of a right parietal GBM (first craniotomy, **left**), tumor recurrence at the site of previous surgery (**centre**), removal of the local tumor recurrence (second craniotomy, **right**).

Due to residual enhancing tissue adjacent to the right lateral ventricle (Fig. 21A, *left*), anti-angiogenic treatment with bevacizumab was initiated (Avastin®, 10 mg/Kg intravenous, every 2 weeks in 6-week cycles). By the third cycle of bevacizumab, follow-up magnetic resonance imaging (MRI) showed reduction of the paraventricular area of contrast enhancement (Fig. 21B, *left*). However, the right temporal lobe appeared swollen due to diffusely infiltrating tissue (Fig. 21B, *right*). After one year, a third craniotomy was performed with resection of the right temporal lobe. Histological examination showed an increased cell density because of enlarged cells with atypical nuclei, which were mainly located along the perivascular spaces (Fig. 21C, *right*).

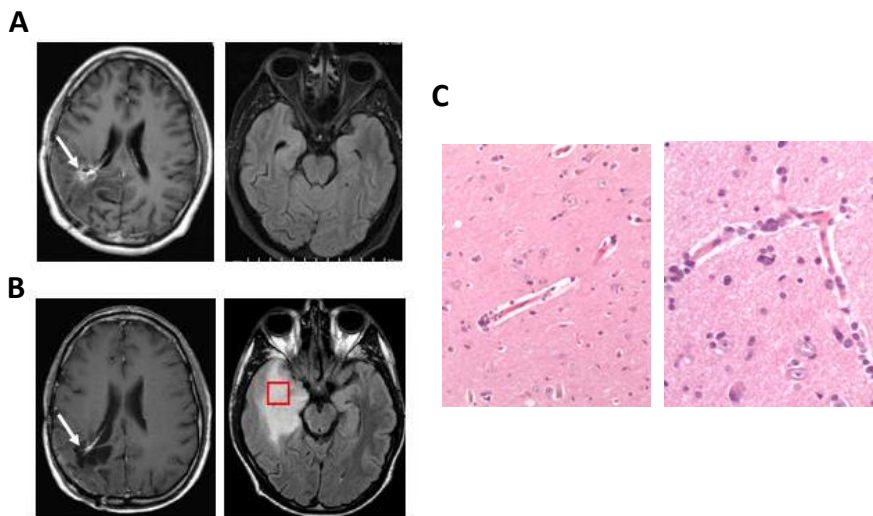


**Figure 21.** **A.** Axial gadolinium-enhanced T1-weighted MR image (**left**) showing an area of contrast enhancement adjacent to the right lateral ventricle (**arrow**). The right temporal lobe shows a normal T2-weighted MR signal (**right**). **B.** Axial gadolinium-enhanced T1-weighted MR image after bevacizumab therapy (**left**) showing disappearance of the contrast enhanced area in the right paraventricular region (**left; arrow**). The right temporal lobe appears swollen due to a hyperintense diffusely infiltrating lesion on T2-weighted MR (**right**). **C.** Histological picture of the resected temporal lobe (brain region framed in **B, right**). The temporal lobe parenchyma appears infiltrated by rare cells with atypical nuclei. Most of these cells are in close relationship with the brain capillaries. Haematoxylin and eosin staining.

Fluorescence microscopy combining fluorescent *in-situ* hybridization (FISH) for *EGFR* and immunohistochemistry for the endothelial marker CD31 showed that a substantial fraction of tumor cells with amplified *EGFR* signals lied close to CD31-expressing endothelial cells (Fig. 22).

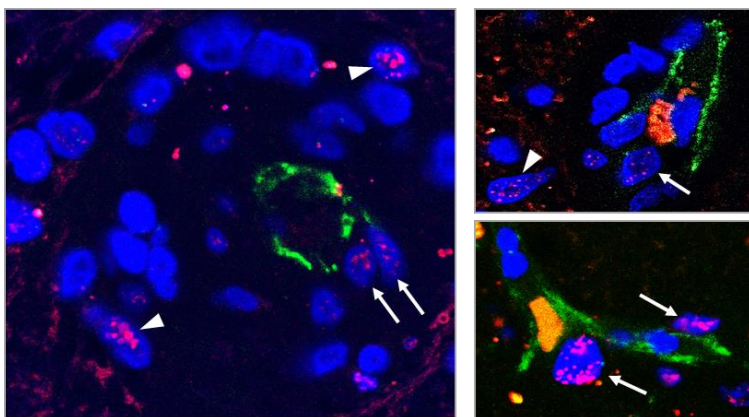


**Figure 22.** Combined anti-CD31 (green) immunohistochemistry and FISH for the *EGFR* probe (red) showing the tumor cell nuclei (blue) with amplified *EGFR* signals either isolated (arrowheads) or in close relationship with CD31<sup>+</sup> endothelial cells (arrows).

Taken together, these results demonstrate that the perivascular spaces are preferential routes for tumor spreading in bevacizumab induced infiltrative shift in GBM.

### **3.2 Effects of bevacizumab on the invasive behavior of U87MG cells *in vitro***

Histological and fluorescence microscopy data of GBM patient previously described, suggest that the infiltrative shift induced by bevacizumab in GBM may involve changes of the perivascular environment, that would become more permissive to the invading tumor cells. Then, in the attempt to reproduce *in vitro* the interaction between GBM cells and perivascular environment, we performed an invasion assay on endothelial cords.

Cords of human HMVECs were established and green fluorescently labeled human GBM U87MG cells, either pretreated with 2.5 mg/ml of IgG or with bevacizumab for 72h, were seeded in the top chamber of a cell invasion assay. Both top and bottom chambers were

additionally treated with either IgG or bevacizumab (final concentration 2.5 mg/mL). We observed that the mere presence of U87MG cells resulted in significant increases of connected tube area, both in wells that received IgG-pretreated U87MG cells and in those with bevacizumab-pretreated U87MG cells. By 48h after seeding, bevacizumab-pretreated cells showed higher invasive growth compared with IgG-pretreated cells (Fig. 23, *right*). Notably, a trend was noted for the bevacizumab-pretreated U87MG cells to line up adjacently to endothelial cords, though there did not appear to be a significant overlapping of U87MG cells with the cords on computerized image analysis. These findings suggest that exposure to bevacizumab may increase the tropism of U87MG cells to the endothelium.

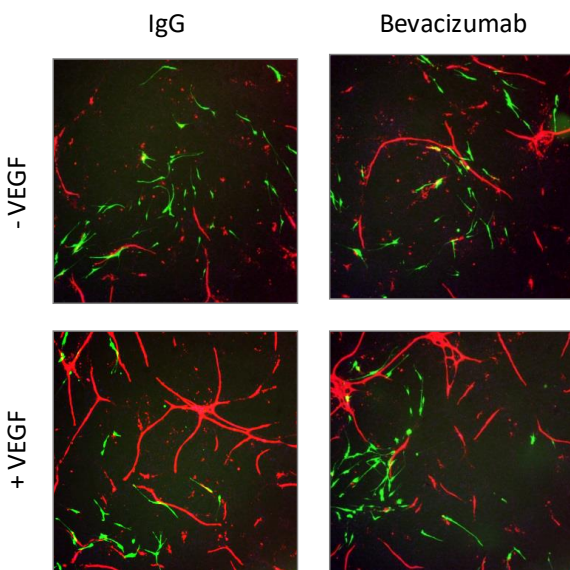


**Figure 23.** Fluorescence microscopy of invasion assay of IgG-pretreated (**left panel**) and bevacizumab-pretreated (**right panel**) U87MG cells, showing an increased tropism of U87MG cells to the endothelium induced by bevacizumab compared to control. The assay was performed either with (**lower panel**) or without (**upper panel**) VEGF (U87MG cells in green, HMVEC-CD31 expressing cells in red).

### 3.3 Effects of bevacizumab on U87MG brain xenografts

In order to reproduce the tumor environment in which bevacizumab induces the infiltrative growth of GBM and further investigate this process, we grafted fluorescently labeled U87MG cells (expressing either m-Cherry or Green Fluorescent Protein, GFP) onto the brain of athymic rats and assessed the effects of bevacizumab on the growth pattern of tumor xenografts. When orthotopically implanted, U87MG cells generate compact tumor masses with sharply defined edges (Fig. 24A-B), without regions of brain infiltration. Small capillaries and venules that crossed the brain-tumor interface were surrounded for short distances by a few tumor cells (Fig. 24C, *right panel*). In peritumor brain regions, the isolated tumor cells that had traveled for longer distances in the brain were found in close relationship with the endothelial cells.

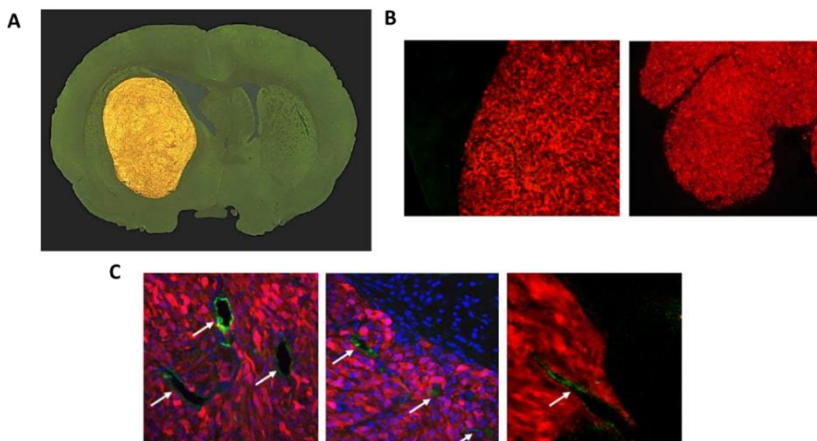


**Figure 24.** **A.** Coronal section through the striatum of U87MG brain xenograft in control rats. **B.** Fluorescence microscopy of tumor margins in control rat (isotype IgG-treated rat, U87MG cells in *red*), showing defined edges. **C.** Immunofluorescence microscopy showing CD31<sup>+</sup> endothelial structures (*green*, arrows) in the core (**left**) and periphery of tumor close to the margin (**centre**). Small capillaries crossing the brain-tumor interface are accompanied by a few tumor cells (*red*) for very short distances (**right**).

---

Bevacizumab-treated tumors were significantly smaller than controls (Fig. 25A). By 28 days after grafting, the tumor volume was  $116.5 \pm 23.1 \text{ mm}^3$  (mean  $\pm$  SEM,  $n=3$ ) and  $17.7 \pm 2.5 \text{ mm}^3$  (mean  $\pm$  SEM,  $n=3$ ) in control and bevacizumab-treated tumors, respectively ( $p<0.02$ ; Student-*t* test). However, metastases were found on the walls of the ventricles in bevacizumab-treated rat brains (Fig. 25A, *arrows*). The margins of bevacizumab-treated tumors were quite irregular with tumor cells that spread onto the surrounding brain (Fig. 25B). By 28 days after grafting, 85.7% of tumor cells that lied farther than  $500 \mu\text{m}$  from the tumor had established cell-to-cell interactions with endothelial elements, whereas in control tumors only rare tumor cells were scattered in the brain up to a maximal distance of  $660 \mu\text{m}$  from the tumor margin (Fig. 25C). Furthermore, we observed that in bevacizumab-treated rats tumor cells arranged to form differently shaped structures, resembling mechanisms of GBM-associated neovascularization such as vessel co-option, tubulogenesis and vascular mimicry (Fig. 25D).

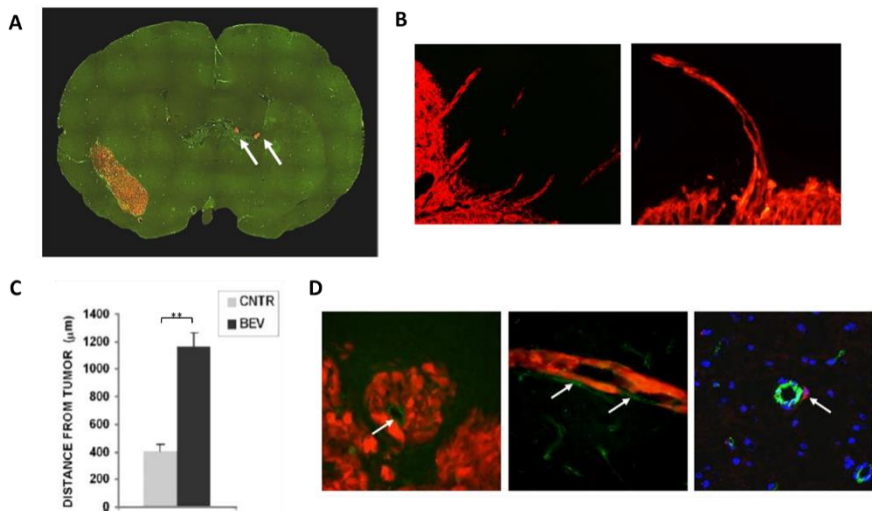


**Figure 25.** **A.** Coronal section through the striatum of U87MG brain xenograft in bevacizumab-treated rats (arrows indicate metastases along the cerebrospinal fluid pathway). **B.** Fluorescence microscopy of tumor margins in bevacizumab-treated rats, showing irregular edges (U87MG cells in red). **C.** Measurement of the distance traveled into the brain by control and bevacizumab-treated tumor cells (\*\* $p<0.01$ ). **D.** Immunofluorescence microscopy showing tumor satellites (red) associated with CD31<sup>+</sup> endothelial structures (**left**, green) suggesting vessel co-option. Chains of tumor cells (red) in single file form mosaic tubules with CD31<sup>+</sup> cells (**centre**, arrows). Isolated m-Cherry U87MG cells distant from the tumor bulk show a strict tropism for the vascular endothelial cells (**right**, arrow).

Therefore, tumor cells after bevacizumab treatment showed a stricter tropism for the vascular endothelial structures than non-treated tumor cells. Altogether, these results demonstrate that the orthotopic U87MG grafting model reproduces bevacizumab-induced infiltrative shift of GBM.

### 3.4 Bevacizumab-induced *in vivo* molecular changes in U87MG

Molecular characterization of the infiltrative shift is required to identify possible mechanisms underlying the development of

bevacizumab-resistance in GBM. Grafting of fluorescent GBM cells allows to recover selectively the tumor cells from the brain xenografts by fluorescent-activated cell sorting (FACS) and then to analyze them at a molecular level. Thus, we evaluated the molecular changes elicited by bevacizumab treatment starting from fluorescent U87MG cells orthotopically implanted in athymic rats. We performed gene expression profiling of fluorescent U87MG cells retrieved by FACS sorting from control and bevacizumab-treated xenografts, in order to identify which genes were modulated by bevacizumab treatment. GSEA of the highest modulated genes revealed that they are mainly associated with epithelial to mesenchymal transition (EMT) signaling pathway (Fig. 26A). Among them, we found the receptor Plexin Domain Containing 1, PLXDC1 (also known as Tumor Endothelial Marker-7, TEM-7), as upregulated in treated cells compared to non-treated cells. PLXDC1 is a trans-membrane protein and it has been demonstrated that it is expressed by the endothelial cells of GBM [101, 102]. To validate PLXDC1 involvement in bevacizumab-induced infiltrative shift, we overexpressed this receptor in U87MG cells. Cytofluorimetric analysis confirmed the overexpression of PLXDC1 (Fig. 26B). Then, we observed that PLXDC1-overexpressing U87MG cells showed increased proliferation and migration abilities *in vitro* compared to GFP-expressing cells used as control (Fig. 26C-D).

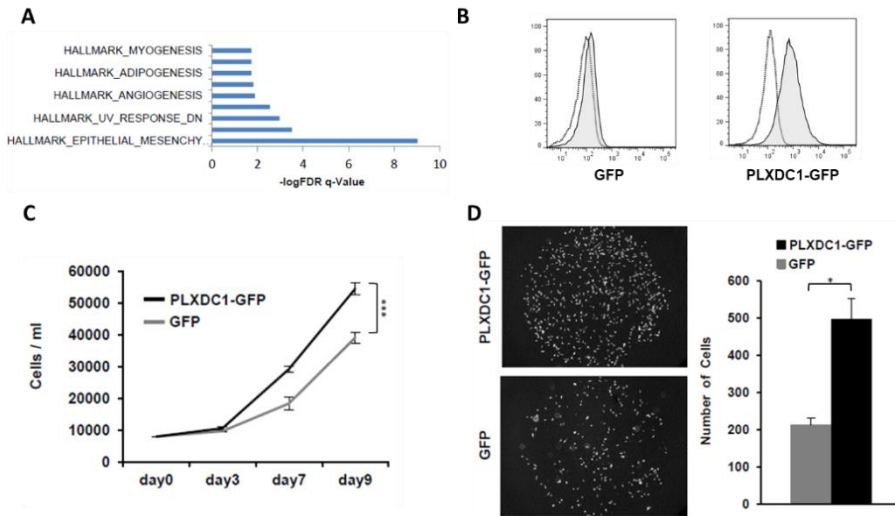


**Figure 26.** **A.** Results of GSEA analysis on gene expression profiles obtained from RNA Affymetrix of U87MG cells retrieved by FACS sorting from control and bevacizumab-treated tumor xenografts. **B.** FACS analysis based on PLXDC1 expression of GFP-expressing (left) and PLXDC1-overexpressing (right) U87MG cells (open histogram = isotype IgG antibody control sample; shaded histogram = anti-PLXDC1 antibody sample). **C-D.** Proliferation (C) and migration (D) assays of GFP-expressing and PLXDC1-overexpressing U87MG cells. Values are mean±SD ( $n=3$ ; \* $p<0.05$ ; \*\*\* $p<0.001$ ).

Furthermore, in *in vivo* experiments PLXDC1-U87MG xenografts showed irregular edges due to vessel co-option and perivascular spreading, differently from GFP-U87MG control xenografts (Fig. 27A-B).

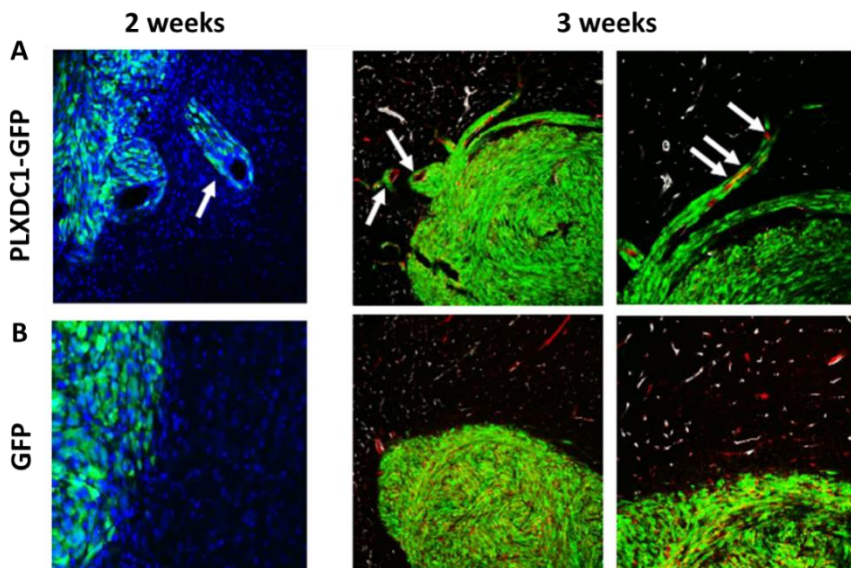


**Figure 27. A-B.** Fluorescence microscopy showing the tendency to form tubular structures and vessel co-option (white arrows) in PLXDC1-overexpressing U87MG brain xenografts (A) compared to control (B; **left panel**, U87MG cells in green, nuclei in blue; **right panel**, U87MG cells in green, immunostaining for the marker for the vascular endothelium lectin in red, coupled with the BBB marker SMI71 in white).

Then, in order to specifically verify its role in bevacizumab-induced infiltrative shift, we downregulated PLXDC1 expression in U87MG cells by short hairpin RNA (shRNA) system (shPLXDC1 U87MG), we established brain xenografts and treated the rats with bevacizumab. Differently from control rats (Fig. 28A, *left*), in which we observed infiltrative growth even after the treatment, shPLXDC1-U87MG brain xenografts did not show tumor spreading along perivascular spaces (Fig. 28A, *centre*). Moreover, combining PLXDC1 downregulation and bevacizumab treatment, we observed a decrease of tumor growth, in addition to the absence of perivascular infiltration (Fig. 28A, *right*), leading to a significant increase in terms

of survival of shPLXDC1 bevacizumab-treated rats compared to the other groups (Fig. 28B).

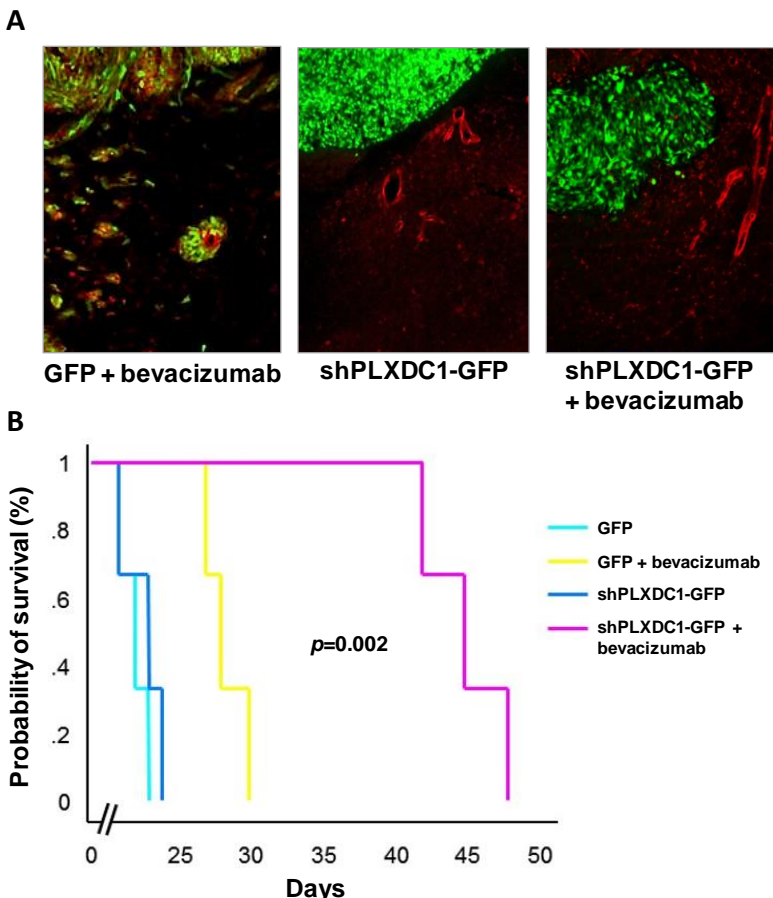


**Figure 28.** **A.** Immunofluorescence showing differences in tumor growth and perivascular infiltration in U87MG brain xenograft control rats after bevacizumab treatment (**left**), shPLXDC1-GFP rats (**centre**) and shPLXDC1-GFP rats after bevacizumab treatment (**right**). (U87MG cells in *green*, staining for lectin in *red*). **B.** Kaplan-Meier curve showing the probability of survival of the different groups of rats compared.

Altogether, these results suggest that PLXDC1 contributes to the perivascular migration observed in bevacizumab-induced infiltrative shift, and its inhibition could enhance the effects of bevacizumab treatment.

### ***3.5 Effects of bevacizumab on GSC brain xenografts***

Since brain xenografts generated through intracerebral injection of GSCs into immunodeficient mice represent the experimental model that closely mimic the parent GBM, we decided to perform the same *in vivo* experiments previously described for U87MG by using GSCs. The tumor xenografts generated by GSC orthotopical injection show highly infiltrative pattern of growth [42, 103, 104], that is one of the main feature of patients' GBM. We injected GFP-expressing GSC#1 onto the striatum of athymic rats and 12 weeks after grafting we administered bevacizumab (10 mg/kg i. p., twice weekly for three weeks). In spite of significant reduction of micro-vessel density, bevacizumab treatment did not inhibit GSC tumor growth to the same extent seen in U87MG xenografts (Fig. 29A). One feature of GSC#1 xenografts was the tendency to form tubular structures. Overall, bevacizumab increased this feature, enhancing perivascular spreading, tubulogenesis and expression of the endothelial markers by the tumor cells, and maintenance of BBB (Fig. 29B).

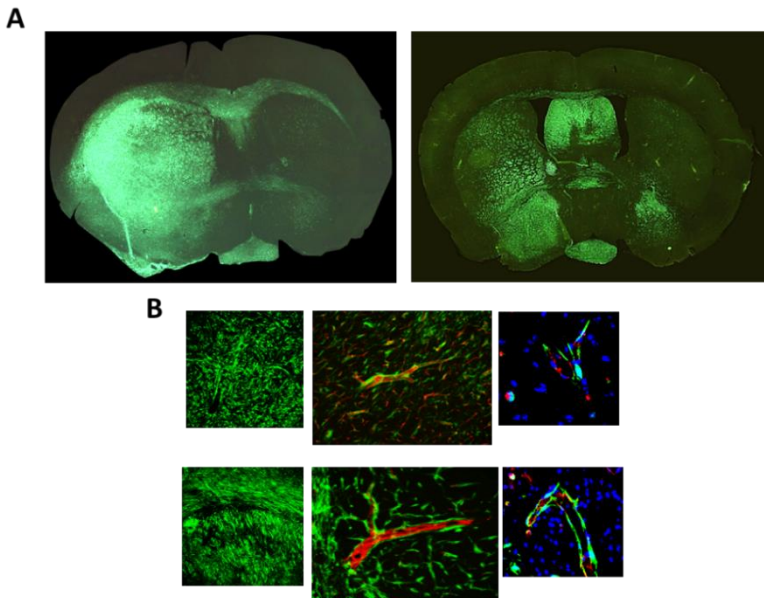


**Figure 29.** **A.** Coronal section through the striatum of isotype IgG- (**left**) and bevacizumab-treated (**right**) GFP-expressing GSC#1 brain xenografts. **B.** Fluorescence microscopy of brain regions with tumor infiltration in isotype IgG- (**upper panel**) and bevacizumab-treated (**lower panel**) rats, showing the tendency to form tubular structures (**left panels**, GSC#1 cells in **green**; **central panels**, immunofluorescence for lectin in **red**; **right panels**, immunofluorescence for the endothelial marker CD31 in **red**).

### 3.6 Bevacizumab-induced *in vivo* molecular changes in GSCs

*In vivo* model allows to highlight the effects of bevacizumab at the cell level in the brain environment. By using the same approach previously described, we retrieved the fluorescently labeled GSCs and performed gene expression profiling after bevacizumab treatment. We identified Plasminogen Activator Urokinase Receptor (PLAUR) and miR-31 among the highest upregulated genes following the treatment, and PLXDC1 as we found in U87MG model. PLAUR encodes the receptor for urokinase plasminogen

activator (uPA) and influences many normal and pathological processes related to cell-surface plasminogen activation and degradation of the extracellular matrix [105]. MiR-31 regulates glioma growth by maintaining cancer stem cells and their niche, and promoting angiogenesis through inhibition of its target, Factor Inhibiting HIF1 (FIH1) [106]. We also found that miR-126, known as a tumor suppressor miRNA in GBM, was highly downregulated in response to bevacizumab treatment *in vivo*. In order to verify *in vitro* the potential role of PLXDC1, PLAUR and miR-31 as targets for blocking the bevacizumab-induced infiltrative growth mediated by GSCs, we overexpressed these genes in GSC#1 cells (data not shown). GSC#1 overexpressing either PLXDC1, PLAUR or miR-31 showed significantly higher clonogenic potential than GFP-expressing cells used as control (Fig. 30).

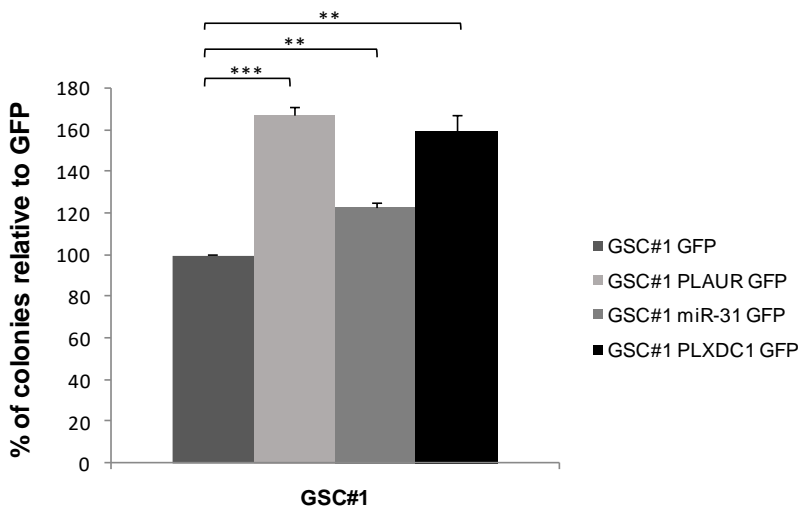


**Figure 30.** Clonogenic assay of GFP-expressing, PLAUR-overexpressing, miR-31-overexpressing and PLXDC1-overexpressing GSC#1. Values are mean±SD ( $n=3$ ; \*\*  $p<0.01$ ; \*\*\*  $p<0.001$ ).

Based on these results, further *in vitro* and *in vivo* experiments will elucidate the role of these genes and the associated signaling pathways in bevacizumab-induced infiltrative growth of GBM mediated by GSCs.

## DISCUSSION

Angiogenesis is a crucial process in GBM maintenance, progression and recurrence, since GBM is a highly angiogenic tumor and one of its main features is a robust neovascularization potential. GBM aggressiveness has also been ascribed to GSCs because of their ability to sustain tumor growth, promote recurrence and the development of therapy resistance. Furthermore, GSCs contribute to GBM neovascularization through different mechanisms. In this study, we focused on the characterization of the molecular mechanisms underlying GBM neovascularization and GSC contribution to this process, in order to improve current anti-angiogenic therapeutic strategies.

Glioblastoma stem-like cells have properties similar to normal neural stem cells (NSCs), such as self-renewal capacity and multilineage differentiation potential. Indeed, GSCs can generate glial and neuronal lineages through transcriptional regulatory networks known to regulate stem cell plasticity and lineage determination under physiological conditions. Like NSCs, it has also been shown that GSCs possess the capacity to trans-differentiate [62-64, 69]. In particular, this process plays an important role in GBM neovascularization, since GSCs trans-differentiate into endothelial cells or pericytes and contribute to form the tumor vasculature. Despite the role of glioblastoma-derived endothelial cells (GdECs) in the pathobiology of GBM has been disputed, different studies demonstrated the importance of targeting endothelial tumor cells [62, 63, 69]. Moreover, in a recent study the biological relevance of GdECs within the tumor has been reinforced. In particular, Hu et al demonstrated that the epigenetic activation of WNT5A, through AKT signaling, drives GSC trans-differentiation into GdECs and

stimulates host EC recruitment to create a vascular niche supporting GSC growth and survival [107]. WNT5A can promote EC lineage differentiation during normal vascular development and can regulate EC proliferation, migration and survival in angiogenesis process [108-110]. It has also been demonstrated that small-molecule activation of WNT signaling generates CD34<sup>+</sup>CD31<sup>+</sup> endothelial progenitor cells that can differentiate into functional ECs [111].

In our *in vitro* model of GSC trans-differentiation, we were able to identify a subpopulation of CD34-expressing cells within the heterogeneous GSC compartment. It might be hypothesized that such CD34<sup>+</sup> cells derived from GSCs are more similar to vascular endothelial progenitor cells than to GSCs, thereby being directly involved in tumor vascularization process because of their differentiation potential into ECs. Therefore, identifying the molecular basis underlying this subpopulation of cells might be important for the development of more specific anti-angiogenic therapies.

MiRNA expression profile analysis provides insights into the characterization of a specific subpopulation of cells, since miRNAs are able to simultaneously modulate multiple genes across different signaling pathways. In our GdECs, miRNA expression profiling revealed a signature of three miRNAs able to clearly distinguish GSCs or GdECs. Gene set enrichment analysis of the three miRNA targets revealed modulation of genes associated with ROS metabolism, angiogenesis, hypoxia, AKT/mTORC1 signaling pathways, among others. It might be hypothesized that inhibiting the most important signaling pathways associated with GSC trans-differentiation and GdEC survival could impair GBM neovascularization. To this aim, we assessed the effect of a collection of kinase inhibitors targeting most cancer-related pathways. Among

the few compounds active at submicromolar concentrations, the oxidative stress inducer Elesclomol showed the most antiproliferative effect on both GSCs and GdECs. Further investigations are required to evaluate the specific signal transduction pathways involved in the sensitivity of these cells to Elesclomol. Evaluation of reverse phase protein array (RPPA)-based pathway-activation profiling in GSCs and GdECs after Elesclomol treatment could provide insights into the molecular mechanisms underlying GSC and GdEC response.

However, it is worth of note that the trans-differentiation process *in vivo* can be affected by several factors within the tumor vascular niche, which can not be reproduced in our GSC trans-differentiation model *in vitro*. Nonetheless, our molecular characterization of GdEC subpopulation can represent the basis for further *in vivo* studies. For these reasons, it will be evaluated if Elesclomol retains its anti-tumor effect *in vivo*, by intracerebral injection of GSCs into immunodeficient mice and subsequent treatment. The preclinical validation of *in vitro* data might provide important information for the use of Elesclomol as novel potential anti-angiogenic strategy, targeting such resistant tumor endothelial cell population responsible of GBM neovascularization process.

Currently, anti-angiogenic therapy in recurrent GBM is represented by the anti-VEGF monoclonal antibody bevacizumab. However, results from recent clinical trials with bevacizumab [85, 86] are openly discordant and in contrast with impressive previous evidence [84]. Moreover, the ability to select the patients who are most likely to benefit and determining the best method of tumor assessment after anti-angiogenic treatment would be ideal to counteract failure of anti-VEGF therapy [112]. In order to investigate the molecular basis of this process, we used our brain xenograft models based on fluorescently labeled GBM cells, either U87MG or GSCs. Our experiments showed that anti-angiogenic treatment induces a

repertoire of vascular-like behaviors by the tumor cells and the acquisition of a stem-like phenotype. Moreover, we were able to identify the most important genes and signaling pathways modulated by bevacizumab treatment. Among them, we identified PLXDC1/TEM-7 as potential target for blocking bevacizumab-induced infiltrative growth and perivascular migration. Bevacizumab treatment of brain tumor xenografts generated by the injection of U87MG cells with downregulation of PLXDC1 led to reduced tumor growth, decreased infiltrative potential and increased survival, differently from the effects of the treatment in control rats. Therefore, our *in vivo* experiments confirmed the role of PLXDC1 in the molecular changes occurring in GBM after bevacizumab treatment. It might be hypothesized that blocking the increased tumor invasiveness elicited by current anti-angiogenic treatment, for example combining bevacizumab with inhibition of PLXDC1, could be adopted as alternative approach to counteract escape mechanisms and development of resistance. Nonetheless, it is worth of note that the most reliable GBM experimental model is represented by brain xenografts generated through intracerebral injection of GSCs into immunodeficient mice. For this reason, based on the results obtained in our *in vivo* GSC model, further experiments will be performed in order to investigate the potential role of PLAUR, miR-31 and miR-126 as molecular players of GSC contribution to bevacizumab-induced infiltrative shift.

Apart from the most common mechanisms of resistance, it is important to take into account alternative escape mechanisms that might explain and contribute to the ineffectiveness of current anti-angiogenic strategy. Extracellular vesicles are emerging as novel potential tools used by tumor cells to counteract anti-angiogenic therapy. A recent study identified a specific high molecular weight of

VEGF-A (VEGF<sub>90K</sub>) that is transported in breast cancer cell-derived microvesicles and if associated with microvesicles makes them less susceptible to the inhibitory action of bevacizumab [113]. Furthermore, it has been reported that cytotoxic stress of tumor cells induced by treatment may enhance the secretion of extracellular vesicles, stimulating angiogenesis and metastasis [114]. Recently, it has been demonstrated that in GBM cells irradiation triggers a phenotypic change, affecting paracrine interactions mediated by microvesicles that promote survival and invasion [115]. The results obtained in our preliminary experiments on GSC- and HMVEC-derived microvesicles showed that irradiation affects microvesicle release. However, in order to verify our hypothesis on the existence of a MV-based crosstalk within the GBM vascular niche, it will be necessary to investigate if microvesicle content is affected by radiations as well. This further characterization will elucidate the potential role of microvesicles in GBM resistance to therapy.

## MATERIALS AND METHODS

### *Cell cultures*

Glioblastoma stem-like cells were isolated from surgical samples of adult GBM patients (WHO grade IV) who had undergone complete or partial surgical resection at the Institute of Neurosurgery, Catholic University School of Medicine in Rome, upon patient informed consent and approval by the local ethical committee. GSC cultures were established from surgical specimens through mechanical dissociation and culturing in a serum-free medium supplemented with 20 ng/ml epidermal growth factor (EGF) and 10 ng/ml basic fibroblast growth factor (bFGF) (Peprotech, Rocky Hill, NY) [42, 43]. Under these conditions, cell lines actively proliferating required 3 to 4 weeks to be established. Tumor cells grow as spheroid clusters (tumorspheres) expressing stem cell markers, such as CD133, sex determining region Y-box 2 (Sox2), Musashi-1 and Nestin. The *in vivo* tumorigenic potential of GBM tumorspheres was assayed by intracranial or subcutaneous cell injection in immunocompromised mice, resulting in tumors with the same antigen expression and histological tissue organization as the human parent tumor [42, 43]. Human microvascular endothelial cell (HMVEC) lines were purchased from Lonza and cultured in endothelial basal medium (EBM-2, Lonza Walkersville Inc., Walkerswill, MD) supplemented with EGM<sup>TM</sup>-2 MV SingleQuots<sup>TM</sup> Kit (Lonza Walkersville Inc.), at 37°C in 5% CO<sub>2</sub> atmosphere. The U87MG human GBM cell line was purchased from the American Type Culture Collection (Manassas, VA) and cultured in DMEM (high glucose, Lonza Milano srl, Milan, Italy) supplemented with 10% heat-inactivated foetal bovine serum, at 37°C in 5% CO<sub>2</sub> atmosphere. M-Cherry red

and GFP fluorescent U87MG cells and GSC lines were obtained by lentiviral infection. For m-Cherry red was used the pLVX-mCherry-C1 vector (Clontech Laboratories, Mountain View, CA); for GFP was used the pRRLsin-cPPT-hCMV-hPGK-GFP-Wpre vector [116].

### ***Plasmid constructs and lentivirus infection***

The PLXDC1 cDNA (NM 020405) and PLAUR cDNA (NM002659) were obtained from total RNA extracted from U87MG cells, retrotranscribed into cDNA by RT-PCR and amplified by qPCR using AccuPrime™ Pfx DNA Polymerase (Thermo Fisher Scientific, Waltham, MA). Primers used for PLXDC1 amplification were: CCATGCGAGGCGAGCTCTGGCT (Forward) and TGTTCTCAGCACTGCTCAGCCTCCATG (Reverse). Primers used for PLAUR amplification were: ACATGGGTACCCGCCGCTG (Forward) and TCAGGTTAGGTCCAGAGGAGAGTGC. The miR-31 precursor was obtained from normal human genomic DNA by amplification by qPCR, using AccuPrime™ Pfx DNA Polymerase (Thermo Fisher Scientific) and the following primers: CACTCTAGAGTCATAGTATTCTCCTGTAACTTGGAAC (Forward) and GCCATGGCCACCTGCATGCCAGTCCCTCGAGTAT (Reverse). RT-PCR analysis was performed using an ABI Prism 7900 Sequence Detector (Applied Biosystems Inc., Carlsbad, CA). The products of amplification were cloned using TA Cloning® Kit (Thermo Fisher Scientific) and then subcloned into GFP lentiviral vector [116] by XbaI-Xho restriction enzymes. The downregulation of PLXDC1 expression in U87MG cells was obtained using pGFP-C-shLenti vector purchased from OriGene (OriGene Technologies, Rockville, MD).

Lentiviral particles were produced by the calcium phosphate transfection protocol in the packaging human embryonic kidney cell line 293T. Briefly, the lentiviral construct was co-transfected with pMDL, pRSV-REV and pSV-G. The calcium-phosphate DNA precipitate was removed after 8h by replacing the medium. Viral supernatants were collected 48h post-transfection, filtered through a 0.45 µm pore size filter and added to U87MG cells or GSCs in the presence of 8 µg/ml polybrene. Cells were centrifuged for 30 minutes at 1800 rpm. After infection, the fluorescence of transduced cells was evaluated by FACSCanto (Becton Dickinson, San Jose, CA).

### ***Trans-differentiation of GSCs***

*In vitro* trans-differentiation of GSCs was performed by culturing GSC tumorspheres in a serum-free medium supplemented with EGM™-2MV SingleQuots™ Kit (Lonza Walkersville Inc.) and 12 µg/ml Bovine Brain Extract (BBE, Lonza Walkersville Inc.) on Matrigel® coated tissue culture surface under hypoxic condition (1% O<sub>2</sub>). Under these conditions, GSCs grow as continuous net-like structures. For the expression of the endothelial markers, cells were incubated for 90 minutes at 4°C with the antibodies, then washed with PBS and analyzed by the flow cytometer FACSCanto (Becton Dickinson). The antibodies used were as follows: anti-CD31-phycoerythrin antibody (1:20, BD Biosciences, Milan, Italy) or PE-conjugated mouse IgG<sub>1</sub> isotype control antibody (Miltenyi Biotec Inc., Bergisch Gladbach, Germany); anti-CD34-phycoerytrin antibody (1:20, clone BIRMA-K3, DakoCytomation, Denmark) or PE-conjugated mouse IgG<sub>1</sub> isotype control antibody (Miltenyi Biotec Inc.). Data were analyzed with FACS Diva software (Becton Dickinson).

### ***Subcutaneous injection of CD34<sup>+</sup> GSCs***

---

After two weeks in endothelial conditions, CD34<sup>+</sup> GSCs were isolated using FACSaria cell sorter (BD Biosciences), obtaining two subpopulations of cells based on CD34 expression levels. Cells were resuspended in cold PBS and the suspension mixed with an equal volume of cold Matrigel. Mice were injected subcutaneously with 0.2 ml of the cell/Matrigel suspension.

### ***MiRNA profiling***

To analyze GSC and GdEC miRNA expression, total RNA was prepared using Qiagen RNeasy Micro Kit (Qiagen, Hilden, Germany). RNA (1 µg) was labeled and hybridized to the Agilent-019118 array (Agilent Technologies, Santa Clara, CA) following the manufacturer's instructions. MiRTarBase was used for miRNA target prediction [117] and gene set enrichment analysis (GSEA) was based on MSigDB using the GSEA online tool [118] hosted by the Broad Institute (<http://www.broadinstitute.org/gsea/index.jsp>).

### ***Drug screening***

For the drug screening experiments, GSCs, GdECs and HMVECs were plated at a density of 1.0x10<sup>4</sup> cells/ml, in triplicate, in a 96-well plate. The FDA-approved kinase inhibitor library (Selleck anti-cancer compound library) and Elesclomol were purchased from Selleckchem (Selleck chemicals, Houston, TX). Compounds were dissolved in DMSO and added 24h after cell plating. After 72h, ATP levels were measured as a surrogate of cell viability using the CellTiter-Glo™ (Promega Inc., Madison, WI) according to the manufacturer's instructions. The mean of the raw luminescence values from triplicate wells treated with vehicle alone (mL<sub>C</sub>), was used as reference to interpolate percent viability from wells treated with drugs (V<sub>D</sub>), using the following formula: V<sub>D</sub>=(L<sub>D</sub>/mL<sub>C</sub>)\*100. [119].

---

### ***Fluorescent labeling of microvesicles***

Microvesicles were labeled using the green fluorescent fatty acid BODIPY® FL C<sub>16</sub> (Thermo Fisher Scientific). To allow the incorporation of the fluorescent molecule as phospholipid into microvesicle membrane, cells were incubated with 10 µM BODIPY for 6h at 37°C in 5% CO<sub>2</sub> atmosphere. Labeling was stopped washing with PBS to remove excess BODIPY.

### ***Exposure of cells to radiations***

Cells at 70% to 80% confluence (density of 1.2x10<sup>5</sup> cells/ml for GSCs) were exposed to single doses of acute cesium-137 (<sup>137</sup>Cs) gamma irradiation (10Gy and 50Gy). Dose rate was 0.8 Gy/min. Media were replaced 4h after irradiation, using exosome-depleted serum for HMVEC (System Biosciences, Palo Alto, CA). Cells were incubated for 40h at 37°C in 5% CO<sub>2</sub> atmosphere before microvesicle isolation.

### ***Microvesicle isolation and count***

Microvesicles were isolated by ultracentrifugation. Cell media were clarified of cells and cellular debris by spinning media at 1400 rpm for 10 minutes, then at 3200 rpm for 20 minutes at 4°C, before pelleting at 33000g for 3h at 4°C. Microvesicles were washed in PBS and repelleted by an additional spinning at 33000g for 3h at 4°C. Labeled microvesicles were resuspended in PBS. Microvesicle count was performed using Gallios flow cytometer (Beckman Coulter Life Sciences, Indianapolis, IN).

### ***Immunoblot analysis on microvesicles***

For the detection of protein markers, microvesicles were resuspended in PBS with protease inhibitor cocktails (Sigma-Aldrich, St. Louis, MO), before boiling in NuPAGE™ LDS Sample Buffer 4x (Thermo

Fisher Scientific) at 95°C for 5 minutes. Protein concentration was quantified using a Bradford protein assay (Bio-Rad Laboratories, Hercules, CA). Seven micrograms of protein were resolved in 10% Tris-Glycine gel and transferred to nitrocellulose membrane overnight at 4°C. Primary antibodies used were as follows: Alix (Cell Signaling Technology Inc., Danvers, MA), tsg101 (Thermo Fisher Scientific). Immunoreactive bands were visualized by using HRP-conjugated secondary antibodies (Sigma-Aldrich) and the ECL system (GE Healthcare, Pittsburgh, PA) and detected using a FluorChem system (ProteinSimple, San Jose, CA).

### ***RNA-Sequencing analysis on microvesicles***

To characterize microvesicle RNA composition, total RNA was extracted from pelleted microvesicles using the miRCURY™ RNA Isolation Kit (Exiqon, Vedbaek, Denmark) according to the manufacturer's instructions. RNA-Sequencing was performed using SMARTer® Small RNA-Seq Kit and SMARTer® Stranded Total RNA-Seq Kit - Pico Input Mammalian (Clontech Laboratories, Mountain View, CA) according to the manufacturer's instructions.

### ***Microvesicle uptake experiments***

To verify labeled microvesicle uptake,  $4 \times 10^4$  cells were incubated with microvesicles (200 MVs/cell) for 1h at 37°C using a thermoblock. Cells were analyzed using the flow cytometer FACSCanto (Beckton Dickinson).

### ***Clinical material***

A surgical specimen of temporal lobe was fixed in formalin and paraffin-embedded. Four- $\mu\text{m}$  thick paraffin sections were de-waxed with xylene and rehydrated in ethanol. After a step of antigen retrieval in microwave oven for 10 minutes in EDTA buffer (1 mM;

pH 8), at 750 W, slides were then incubated with monoclonal mouse anti-human CD31 (Clone JC70A; 1:50, Dako, High Glostrup, Denmark) in a humidified box for 60 minutes at room temperature. Slides were washed twice in PBS 1x (pH 7.4) and incubated with anti-human IgG (Fab specific)-FITC antibody (Vector Laboratories, Burlingame, CA) 1:200 for 60 minutes at room temperature in the dark. After immunofluorescence staining, slides were rinsed three times for 5 minutes each in PBS/0.5% Tween 20 and then were dehydrated in alcohol, and allowed to completely air dry. 10 µl of Vysis LSI EGFR SpectrumOrange/CEP 7 SpectrumGreen probes solution (Vysis EGFR/CEP 7 FISH Probe Kit, Vysis Inc, AbbotLaboratories SA, Downers Grove, IL) were added to each slides. The probes and target DNA were co-denatured at 71°C for 5 minutes followed by hybridization overnight at 37°C. Post-hybridization process included subsequent washing in 0.2x SSC/0.3% NP40 for 2 minutes at 73°C and in 2x SSC/0.1% NP40 for 1 minute at room temperature. Slides were counterstained with DAPI (Vectashield mounting medium with Dapi, Vector Laboratories). Images were captured using a Laser Scanning Confocal Microscope (IX81, Olympus Inc, Melville, NY).

### ***In vitro assessment of cell motility and invasion***

Invasion assay on endothelial cords was performed as previously described [120]. Briefly, HMVECs were plated at  $5 \times 10^4$  cells/well into 96-well black poly-D lysine coated plates (BD Biosciences). After 24h,  $5 \times 10^3$  GFP expressing U87MG cells per well, either pretreated with 2.5 mg/ml of IgG or with bevacizumab for 72h, were over-seeded. Additional treatment with either IgG or bevacizumab occurred 4 hours following U87MG cells plating. Where applicable, 10 ng/ml VEGF (Invitrogen) were added simultaneously with IgG or bevacizumab. Cells were directly fixed for 10 min with 3.7% formaldehyde (Sigma Aldrich) followed by ice-cold 70% ethanol for

30 min at 25°C. Cells were rinsed once with PBS, blocked for 30 min with 1% BSA, and immunostained for 1 hour with monoclonal mouse anti-human CD31 (Clone JC70A; 1:50, Dako). Cells were washed 3 times with PBS and incubated with Alexa Fluor® 546 goat anti-human secondary antibody (1:500; Thermo Fisher Scientific) for 2 hours at room temperature in the dark. Immunofluorescence was observed with a laser confocal microscope (SP5; Leica, Wetzlar, Germany).

### ***Intracranial xenografts of fluorescent human GBM tumor cells***

Immunosuppressed athymic rats (male, 250-280g; Charles River, Milan, Italy) were anesthetized with intraperitoneal injection of diazepam (2 mg/100g) followed by intramuscular injection of ketamine (4 mg/100g). Animal skulls were immobilized in a stereotactic head frame and a burr hole was made 3 mm right of the midline and 2 mm anterior to the bregma. The tip of a 10 µl-Hamilton microsyringe was placed at a depth of 5 mm from the dura and m-Cherry/GFP U87MG cells or GFP GSC#1 were slowly injected. After grafting, the animals were kept under pathogen-free conditions in positive-pressure cabinets (Tecniplast Gazzada, Varese, Italy) and observed daily for neurological signs. Beginning 4 days after implantation of U87MG cells and 12 weeks after implantation of GSCs, the rats were treated with bevacizumab (10 mg/kg i.p.) twice weekly for three weeks. Control animals were treated with PBS. After 28 days of survival of U87MG xenograft bearing rats and 16 weeks for GSC xenograft bearing rats, the animals were deeply anesthetized and transcardially perfused with 0.1M PBS (pH 7.4) then treated with 4% paraformaldehyde in 0.1M PBS. The brain was removed and stored in 30% sucrose buffer overnight at 4° C.

### ***Fluorescence microscopy and immunofluorescence of brain tumor xenografts***

The brains were serially cryotomed at 20 µm on the coronal plane. Sections were collected in distilled water and mounted on slides with Vectashield mounting medium (Bio-Optica, Milan, Italy). Images were acquired with a laser scanning confocal microscope (LSM 500 META, Zeiss, Milan, Italy). The cranio-caudal extension of the brain tumor was assessed on serial coronal sections. The tumor volume was determined according to the equation:  $V = (a^2 \times b)/2$ , where  $a$  is the mean transverse diameter of the tumor calculated on coronal sections through the tumor epicenter and  $b$  is the cranio-caudal extension of the tumor [120]. For immunofluorescence, coronal sections of the brain (40 µm thick) were blocked in PBS with 10% BSA, 0.3% Triton X-100 for 45 minutes. Sections were incubated overnight at 4 °C with primary antibodies in PBS with 0.3% Triton X-100 and 0.1% normal donkey serum (NDS). Monoclonal antibodies used were as follows: anti-rabbit Ki-67 (1:150, Thermo Fisher Scientific), mouse anti-Rat Blood-Brain Barrier (Clone SMI-71) (1:500; Biolegend, San Diego, CA). Polyclonal antibodies used were as follows: goat anti-CD34 (C-18) (1:50; Santa Cruz biotechnology, Dallas, TX), rat anti-mouse CD31 (1:100) (BD Bioscience, Franklin Lakes, NJ), rabbit anti-GFAP (1:1000; Dako Italia, Milan, Italy). For detecting brain microvessels, sections were incubated overnight at 4°C in PBS with 0.3% Triton X-100 and 0.1% NDS with Lectin from Lycopersicon esculentum (tomato) biotin conjugate (1:500; Sigma-Aldrich) together with primary antibodies. Slices were rinsed and incubated in PBS containing 0.3% Triton X-100 with secondary antibodies for 2 hours at RT. Secondary antibodies used were as follows: Alexa Fluor® 647 or 555 or 488 donkey anti-mouse, Alexa Fluor® 488 or 555 or 647, donkey anti-

rabbit secondary antibodies (1:500; Thermo Fisher Scientific), Alexa Fluor® 488 or 555 donkey anti-goat antibodies (1:400; Thermo Fisher Scientific), Cy3 donkey anti-Rat (1:200, EMD Millipore, Billerica, MA). For lectin immunostaining, sections were incubated for 2 hours at RT in PBS containing 0.3% Triton X-100 with streptavidin protein, DyLight 405 conjugate or streptavidin Alexa Fluor® 647 conjugate (1:200; Thermo Fisher Scientific). Before mounting, slices were incubated with DAPI (1:4000; Sigma-Aldrich) for 10 minutes. Immunofluorescence was observed with a laser confocal microscope (SP5; Leica) and images were acquired. Image analysis was performed with Leica Application Suite X software.

### ***Genomic profiling of U87MG cells and GSC#1 after in vivo treatment with bevacizumab***

Twenty-eight days after intracerebral grafting of U87MG cells or sixteen weeks after intracerebral grafting of GSC#1, the brain of rats treated either with bevacizumab or with saline were removed, and mechanically dissociated to obtain single cell suspensions. The fluorescent m-Cherry U87MG cells and GFP GSC#1 were isolated by using FACSaria cell sorter (BD Biosciences). Total RNA was extracted from cells using TRIzol reagent (Life Technologies Corporation, Carlsbad, CA), labeled and hybridized to the Affymetrix GeneChip1.0ST array (Affymetrix, Santa Clara, CA) according to the manufacturer's instructions. Data preprocessing prior to the formal statistical analysis involved standard processes of normalization [robust Multi-array Average (RMA) method]. All data analysis was performed with R (<http://www.R-project.org>) using Bioconductor [121]. Differentially regulated genes were determined with LIMMA [123] applying default parameters and a FDR-corrected *p* value cut-off <0.05. Generation of the unified dataset

involved two consecutive steps. Gene set enrichment analysis was based on MSigDB using the GSEA online tool [118] hosted by the Broad Institute (<http://www.broadinstitute.org/gsea/index.jsp>).

### ***Cell growth, migration and colony formation***

For proliferation assay, GFP and PLXDC1-GFP U87MG cells were plated at a density of  $8 \times 10^4$  cells/ml in 96 well plates in triplicate. Cell proliferation was monitored by counting the cells and confirmed by using the CellTiter-Blue™ Viability Assay (Promega Inc.). The motility of transduced U87MG cells was evaluated by plating in Corning FluoroBlok™ Multiwell Inserts System (Corning Life Sciences, Tewksbury, MA), according to the manufacturer's instruction. Briefly,  $1 \times 10^3$  cells were added to the upper chambers in DMEM medium without serum. FBS completed medium was used as chemoattractant in the lower wells. The plates were incubated for 48h at 37°C, after which the fluorescent dye calcein acetoxyethyl ester (calcein AM, Life Technologies Corporation) was added to the lower chamber for 30 min. The cell viability indicator calcein AM is a non-fluorescent, cell permeant compound that is hydrolyzed by intracellular esterases into the fluorescent anion calcein and can be used to fluorescently label viable cells before microscope observation. The number of migrated cells was evaluated by counting the cells after imaging acquisition using a fluorescence microscope.

Colony formation ability was evaluated by plating a single cell/well in 96 well plates. After 3-4 weeks, each well was examined and the number of spheres/cell aggregates were counted.

### ***Statistical analysis***

GraphPad prism version 4.0 (GraphPad Software, La Jolla, CA, [www.graphpad.com](http://www.graphpad.com)) was used for plots of the library screening. Statistical significance was assessed by a two-tailed Student's *t*-test with equal variance between groups, and assigned to *p*-values <0.05. Asterisks reported in the plots indicate the level of significance as follows: single asterisks for *p*<0.05, two asterisks for *p*<0.01 and three asterisks for *p*<0.001.

## REFERENCES

- [1] Alifieris C., Trafalis D.T. Glioblastoma multiforme: Pathogenesis and treatment. *Pharmacology & Therapeutics*, 152; 63-82 (2015).
- [2] Schwartzbaum J.A., Fisher J.L., Aldape K.D., et al, Epidemiology and molecular pathology of glioma. *Nature Clinical Practice. Neurology*, 2; 494-503 (2006).
- [3] Stupp R., Hegi M.E., Neyns B., et al. Phase I/II a study of cilengitide and temozolomide with concomitant radiotherapy followed by cilengitide and temozolomide maintenance therapy in patients with newly diagnosed glioblastoma. *Journal of Clinical Oncology*, 28; 2712-2718 (2010).
- [4] Ostrom Q. T., Gittleman H., Farah P., et al. CBTRUS statistical report: primary brain and central nervous system tumors diagnosed in the United States in 2006–2010. *Neuro-Oncology*, 15 (6); 1-56 (2013).
- [5] Ohgaki H., Kleihues P., Epidemiology and etiology of gliomas, *Acta Neuropathologica*, 109; 93-108 (2005).
- [6] Kim S.S., Harford J.B., Pirolo K.F., et al. Effective treatment of glioblastoma requires crossing the blood-brain barrier and targeting tumors including cancer stem cells: The promise of nanomedicine. *Biochemical and Biophysical Research Communications*, 468; 485-489 (2015).
- [7] Urbańska K., Sokołowska J., Szmidt M., et al. Glioblastoma multiforme – an overview. *Contemporary Oncology*, 18; 307-312 (2014).
- [8] Karcher S., Steiner H.H., Ahmadi R., et al. Different angiogenic phenotypes in primary and secondary glioblastomas. *International Journal of Cancer*, 118; 2182-2189 (2006).
- [9] Miranda A., Blanco-Prieto M., Sousa J., et al. Breaching barriers in glioblastoma. Part I: Molecular pathways and novel treatment

- approaches. *International Journal of Pharmaceutics*, <http://dx.doi.org/10.1016/j.ijpharm.2017.07.056>
- [10] Auffinger B., Spencer D., Pytel P., et al. The role of glioma stem cells in chemotherapy resistance and glioblastoma multiforme recurrence. *Expert Review of Neurotherapeutics*, 15; 741-752 (2015).
- [11] Stupp R., Mason W.P., van den Bent M.J., et al. Radiotherapy plus concomitant and adjuvant temozolomide for glioblastoma. *The New England Journal of Medicine*, 352; 987-996 (2005).
- [12] Aldape K., Zadeh G., Mansouri S., et al. Glioblastoma: pathology, molecular mechanisms and markers. *Acta Neuropathologica*, 129 (6); 829-48 (2015).
- [13] Lu J., Cowperthwaite M.C., Burnett M.G., et al. Molecular predictors of long-term survival in Glioblastoma Multiforme patients. *PloS ONE*, 11 e0154313 (2016).
- [14] The Cancer Genome Atlas (TCGA) Research Network: Comprehensive genomic characterization defines human glioblastoma genes and core pathways. *Nature*, 455; 1061-1068 (2008).
- [15] Dunn G. P., Rinne M. L., Wykosky J., et al. Emerging insights into the molecular and cellular basis of glioblastoma. *Genes and Development*, 26; 756-784 (2012).
- [16] Koul D. PTEN signaling pathways in glioblastoma. *Cancer Biology and Therapy*, 7; 1321-1325 (2008).
- [17] Crespo I., Vital A. L., Gonzalez-Tabla M., et al. Molecular and genomic alterations in Glioblastoma Multiforme. *The American Journal of Pathology*, 185; 1820-1833 (2015).
- [18] Hanahan D., Weinberg R. A. Hallmarks of cancer: the next generation. *Cell*, 144; 646-674 (2011).
- [19] Reya T., Morrison S. J., Clarke M. F., et al. Stem cells, cancer, and cancer stem cells. *Nature*, 414; 105–111 (2001).
- [20] Vermeulen L., de Sousa E Melo F., Richel D. J., et al. The developing cancer stem-cell model: clinical challenges and opportunities. *The Lancet Oncology*, 13; 83-89 (2012).
-

- [21] Vermeulen L., de Sousa E Melo F., van der Heijdon M., et al. Wnt activity defines colon cancer stem cells and is regulated by the microenvironment. *Nature Cell Biology*, 12; 468-476 (2010).
- [22] Liu S., Ginestier C., Ou S. J., et al. Breast cancer stem cells are regulated by mesenchymal stem cells through cytokine networks. *Cancer Research*, 71; 614-624 (2011).
- [23] Calabrese C., Poppleton H., Kocak M., et al. A perivascular niche for brain tumor stem cells. *Cancer Cell*, 11; 69-82 (2007).
- [24] Ignatova T. N., Kukekov V. G., Laywell E. D., et al.. Human cortical glial tumors contain neural stem-like cells expressing astroglial and neuronal markers in vitro. *Glia*, 39; 193-206 (2002).
- [25] Hemmati H. D., Nakano I., Lazareff J. A., et al. Cancerous stem cells can arise from pediatric brain tumors. *Proceedings of the National Academy of Science U.S.A.*, 100; 15178-15183 (2003).
- [26] Singh S. K., Clarke I. D., Terasaki M., et al. Identification of a cancer stem cell in human brain tumors. *Cancer Research*, 63; 5821-5828 (2003).
- [27] Singh S. K., Hawkins C., Clarke I. D., et al. Identification of human brain tumour initiating cells. *Nature*, 432; 396-401 (2004).
- [28] Galli R., Binda E., Orfanelli U., et al. Isolation and characterization of tumorigenic, stem-like neural precursors from human glioblastoma. *Cancer Research*, 64; 7011-7021 (2004).
- [29] Uchida N., Buck D. W., He D., et al. Direct isolation of human central nervous system stem cells. *Proceedings of the National Academy of Science U.S.A.*, 97; 14720-14725 (2000).
- [30] Lathia J. D., Mack S. C., Mulkearns-Hubert E. E., et al. Cancer stem cells in glioblastoma. *Genes and Development*, 29; 1203-1217 (2015).
- [31] Goodell M. A., Brose K., Paradis G., et al. Isolation and functional properties of murine hematopoietic stem cells that are replicating in vivo. *The Journal of Experimental Medicine*, 183; 1797-1806 (1996).

- [32] Kondo T., Setoguchi T., Taga T. Persistence of a small subpopulation of cancer stem-like cells in the C6 glioma cell line. *Proceedings of the National Academy of Science U.S.A.*, 101: 781-786 (2004).
- [33] Auffinger B., Tobias A. L., Han Y., et al. Conversion of differentiated cancer cells into cancer stem-like cells in a glioblastoma model after primary chemotherapy. *Cell Death and Differentiation*, 21; 1119-1131 (2014).
- [34] Bao S., Wu Q., McLendon R. E., et al. Glioma stem cells promote radioresistance by preferential activation of the DNA damage response. *Nature*, 444; 756-760 (2006).
- [35] Chen J., Li Y., Yu T. S., et al. A restricted cell population propagates glioblastoma growth after chemotherapy. *Nature*, 488; 522-526 (2012).
- [36] Annovazzi L., Mellai M., Schiffer D. Chemotherapeutic drugs: DNA damage and repair in glioblastoma. *Cancers*, 9, 57; doi: 10.3390/cancers9060057 (2017).
- [37] Sottoriva A., Spiteri I., Piccirillo S. G., et al. Intratumor heterogeneity in human glioblastoma reflects cancer evolutionary dynamics. *Proceedings of the National Academy of Science U.S.A.*, 110; 4009-4014 (2013).
- [38] Patel A. P., Tirosh I., Trombetta J. J., et al. Single-cell RNA-seq highlights intratumoral heterogeneity in primary glioblastoma. *Science* 344; 1396-1401 (2014).
- [39] Al Hajj M., Becker M. W., Wicha M., et al. Therapeutic implications of cancer stem cells. *Current Opinion in Genetics and Development*, 14; 43-47 (2004).
- [40] Sottoriva A., Verhoeff J. J., Borovski T., et al. Cancer stem cell tumor model reveals invasive morphology and increased phenotypical heterogeneity. *Cancer Research*, 70; 46-56 (2010).
- [41] Sottoriva A., Vermeulen L., Tavare S. Modeling evolutionary dynamics of epigenetic mutations in hierarchically organized tumors. *PLoS Computational Biology*, 7; e1001132 (2011).

- [42] Pallini R., Ricci-Vitiani L., Banna G. L., et al. Cancer stem cell analysis and clinical outcome in patients with glioblastoma multiforme. *Clinical Cancer Research*, 14; 8205-8212 (2008).
- [43] D'Alessandris Q. G., Biffoni M., Martini M., et al. The clinical value of patient-derived glioblastoma tumorspheres in predicting treatment response. *Neuro-Oncology*, 19 (8); 1097-1108. (2017).
- [44] W. Risau, I. Flamme. Vasculogenesis. *Annual Review of Cell and Developmental Biology*, 11; 73-91 (1995).
- [45] J. Folkman, Y. Shing. Angiogenesis. *The Journal of Biological Chemistry*, 267; 10931-10934 (1992).
- [46] Plate K.H., Scholz A., Dumont D.J. Tumor angiogenesis and anti-angiogenic therapy in malignant gliomas revisited. *Acta Neuropathologica*, 124; 763-775 (2012).
- [47] Jhaveri N., Chen T. C., Hofman F. M. Tumor vasculature and glioma stem cells: Contributions to glioma progression. *Cancer Letters*, 380; 545-551 (2016).
- [48] Ferrara N. VEGF and the quest for tumour angiogenesis factors. *Nature Reviews Cancer*, 2; 795-803 (2002).
- [49] Greenblatt M., Shubick P. Tumor angiogenesis: transfilter diffusion studies in the hamster by the transparent chamber technique. *Journal of the National Cancer Institute*, 41; 111-124 (1968).
- [50] Ehrmann R.L., Knoth M. Choriocarcinoma. Transfilter stimulation of vasoproliferation in the hamster cheek pouch. Studied by light and electron microscopy. *Journal of the National Cancer Institute*, 41; 1329-1341 (1968).
- [51] Folkman J. Tumor angiogenesis: therapeutic implications. *The New England Journal of Medicine*, 285; 1182-1186 (1971).
- [52] Jain R.K., di Tomaso E., Duda D.G., et al. Angiogenesis in brain tumours. *Nature Reviews Neuroscience*, 8; 610-622 (2007).
- [53] Kleihues P., Cavenee W. K, International Agency for Research on Cancer. *Pathology and Genetics of Tumours of the Nervous System* (2000).
-

- [54] Carmeliet P., Jain R. K. Angiogenesis in cancer and other diseases. *Nature*, 407; 249-257 (2000).
- [55] van Beijnum J. R., Nowak-Sliwinska P., Huijbers E. J. M., et al. The Great Escape; the Hallmarks of Resistance to Antiangiogenic Therapy. *Pharmacological Reviews*, 67; 441-461 (2015).
- [56] Hardee M. E., Zagzag D. Mechanisms of glioma-associated neovascularization. *The American Journal of Pathology*, 181; 1126-1141 (2012).
- [57] Holash J., Maisonpierre P. C., Compton D., et al. Vessel cooption, regression, and growth in tumors mediated by angiopoietins and VEGF. *Science*, 284; 1994-1998 (1999).
- [58] Zagzag D., Amirnovin R., Greco M. A., et al. Vascular apoptosis and involution in gliomas precede neovascularization: a novel concept for glioma growth and angiogenesis. *Laboratory Investigation*, 80; 837-849 (2000).
- [59] Brem S. The role of vascular proliferation in the growth of brain tumors. *Clinical Neurosurgery*, 23; 440-453 (1976).
- [60] Kioi M., Vogel H., Schultz G., et al. Inhibition of vasculogenesis, but not angiogenesis, prevents the recurrence of glioblastoma after irradiation in mice. *The Journal of Clinical Investigation*, 120; 694-705 (2010).
- [61] Maniotis A. J., Folberg R., Hess A., et al. Vascular channel formation by human melanoma cells in vivo and in vitro: vasculogenic mimicry. *The American Journal of Pathology*, 155; 739-752 (1999).
- [62] Ricci-Vitiani L., Pallini R., Biffoni M., et al. Tumour vascularization via endothelial differentiation of glioblastoma stem-like cells. *Nature*, 468 (7325); 824-828 (2010).
- [63] Wang R., Chadalavada K., Wilshire J., et al. Glioblastoma stem-like cells give rise to tumour endothelium. *Nature*, 468 (7325); 829-833 (2010).

- [64] Cheng L., Huang Z., Zhou W., et al. Glioblastoma stem cells generate vascular pericytes to support vessel function and tumor growth. *Cell*, 153; 139-152 (2013).
- [65] Bao S., Wu Q., Sathornsumetee S., et al. Stem cell-like glioma cells promote tumor angiogenesis through vascular endothelial growth factor. *Cancer Research*, 66; 7843-7848 (2006).
- [66] Folkins C., Shaked Y., Man S., et al. Glioma tumor stem-like cells promote tumor angiogenesis and vasculogenesis via vascular endothelial growth factor and stromal-derived factor 1. *Cancer Research*, 69; 7243-7251 (2009).
- [67] Galan-Moya E.M., Le Guelte A., Lima Fernandes E., et al. Secreted factors from brain endothelial cells maintain glioblastoma stem-like cell expansion through the mTOR pathway. *EMBO Reports*, 12470-12476 (2011).
- [68] Galan-Moya E.M., Treps L., Oliver L., et al. Endothelial secreted factors suppress mitogen deprivation-induced autophagy and apoptosis in glioblastoma stem-like cells. *PLoS ONE*, 9; e93505 (2014).
- [69] Soda Y., Marumoto T., Friedmann-Morvinski D., et al. Transdifferentiation of glioblastoma cells into vascular endothelial cells. *Proceedings of the National Academy of Science U.S.A.*, 108; 4274-4280 (2011).
- [70] Piccirillo S.G., Combi R., Cajola L., et al. Distinct pools of cancer stem-like cells coexist within human glioblastomas and display different tumorigenicity and independent genomic evolution. *Oncogene*, 28; 1807-1811 (2009).
- [71] Yanez-Mo M., Siljander P. R. M., Andreu Z., et al. Biological properties of extracellular vesicles and their physiological functions. *Journal of Extracellular Vesicles*, 14; 27066 (2015).
- [72] Skog J., Wurdinger T., van Rijn S., et al. Glioblastoma microvesicles transport RNA and protein that promote tumor growth and provide diagnostic biomarkers. *Nature Cell Biology*, 10 (12); 1470-1476 (2008).
-

- [73] Kucharzewska P., Christianson H. C., Welch J. E., et al. Exosomes reflect the hypoxic status of glioma cells and mediate hypoxia-dependent activation of vascular cells during tumor development. *Proceedings of the National Academy of Science U.S.A.*, 110 (18); 7312-7317 (2013).
- [74] Jain R. K., Carmeliet P. Snapshot: tumor angiogenesis. *Cell*, 149; 1408e1 (2012)
- [75] Butler J. M., Kobayashi H., Rafii S. Instructive role of the vascular niche in promoting tumour growth and tissue repair by angiocrine factors. *Nature Reviews Cancer*, 10; 138-146 (2010).
- [76] Griffioen A. W., Molema G. Angiogenesis: potentials for pharmacologic intervention in the treatment of cancer, cardiovascular diseases, and chronic inflammation. *Pharmacological Reviews* 52; 237-268 (2000).
- [77] Weis S. M., Cheresh D. A. Tumor angiogenesis: molecular pathways and therapeutic targets. *Nature Medicine*, 17; 1359-1370 (2011).
- [78] Jain R. K. Normalization of tumor vasculature: an emerging concept in antiangiogenic therapy. *Science*, 307 (5706); 58-62 (2005).
- [79] De Bock K., Cauwenberghs S., Carmeliet P. Vessel abnormalization: another hallmark of cancer? Molecular mechanisms and therapeutic implications. *Current Opinion in Genetics and Development*, 21 (1); 1-7 (2010).
- [80] Vasudev N. S., Reynolds A. R. Anti-angiogenic therapy for cancer: current progress, unresolved questions and future directions. *Angiogenesis*, 17; 471-494 (2014).
- [81] Carmeliet P., Jain R. K. Molecular mechanisms and clinical applications of angiogenesis. *Nature*, 473 (7347); 298-307 (2011).
- [82] Arbab A. S. Activation of alternative pathways of angiogenesis and involvement of stem cells following anti-angiogenesis treatment in glioma. *Histology and Histopathology*, 27 (5); 549-557 (2012).

- [83] Ulbricht L. K., Matschke U., Brockmann J., et al. Levels of soluble vascular endothelial growth factor (VEGF) receptor 1 in astrocytic tumors and its relation to malignancy, vascularity, and VEGF-A. *Clinical Cancer Research*, 9; 1399-1405 (2003).
- [84] Cohen M. H., Shen Y. L., Keegan P., et al. FDA drug approval summary: bevacizumab (Avastin) as treatment of recurrent glioblastoma multiforme. *Oncologist*, 14; 1131-1138 (2009).
- [85] Chinot O. L., Wick W., Mason W., et al. Bevacizumab plus radiotherapy-temozolomide for newly diagnosed glioblastoma. *The New England Journal of Medicine*, 370; 709-722 (2014).
- [86] Gilbert M. R., Dignam J. J., Armstrong T. S., et al., A randomized trial of bevacizumab for newly diagnosed glioblastoma, *The New England Journal of Medicine*, 370; 699-708 (2014).
- [87] de Groot J. F., Fuller G., Kumar A. J., et al. Tumor invasion after treatment of glioblastoma with bevacizumab: radiographic and pathologic correlation in humans and mice. *Neuro-Oncology*, 12 (3); 233-242 (2010).
- [88] Norden A. D., Young J. S., Setayesh K., et al. Bevacizumab for recurrent malignant gliomas: efficacy, toxicity, and patterns of recurrence. *Neurology*, 70 (10); 779-787 (2008).
- [89] Du R., Lu K. V., Petritsch C., et al. HIF-1  $\alpha$  induces the recruitment of bone marrow-derived vascular modulatory cells to regulate tumor angiogenesis and invasion. *Cancer Cell*, 13; 206-220 (2008).
- [90] Piao Y., Liang J., Holmes L., et al. Acquired resistance to anti-VEGF therapy in glioblastoma is associated with a mesenchymal transition. *Clinical Cancer Research*, 19; 4392-4403 (2013).
- [91] Piao Y., Liang J., Holmes L., et al. Glioblastoma resistance to anti-VEGF therapy is associated with myeloid cell infiltration, stem cell accumulation, and a mesenchymal phenotype. *Neuro-Oncology*, 14; 1379-1392 (2012).

- [92] Falchetti M. L., Pierconti F., Casalbore P., et al. Glioblastoma induces vascular endothelial cells to express telomerase *in vitro*. *Cancer Research*, 63; 3750-3754 (2003).
- [93] Bachetti T., Morbidelli L. Endothelial cells in culture: a model for studying vascular functions. *Pharmacological Research*, 42 (1); 9-19 (2000).
- [94] Sidney L. E., Branch M. J., Dunphy S. E., et al. Concise review: evidence for CD34 as a common marker for diverse progenitors. *Stem Cells*, 32; 1380-1389 (2014).
- [95] Kirshner J. R., He S., Balasubramanyam V., et al. Elesclomol induces cancer cell apoptosis through oxidative stress. *Molecular Cancer Therapeutics*, 7; 2319-2327 (2008).
- [96] Park J. E., Tan H. S., Datta A., et al. Hypoxic tumor cell modulates its microenvironment to enhance angiogenic and metastatic potential by secretion of proteins and exosomes. *Molecular Cell Proteomics*, 9; 1085-1099 (2010).
- [97] King H. W., Michael M. Z., Gleadle J. M. Hypoxic enhancement of exosome release by breast cancer cells. *BMC Cancer*, 12; 421 (2012).
- [98] Arscott W. T., Tandle A. T., Zhao S., et al. Ionizing radiation and glioblastoma exosomes: implications in tumor biology and cell migration. *Translational Oncology*, 6; 638-648 (2013).
- [99] Pàez-Ribes M., Allen E., Hudock J., et al. Antiangiogenic therapy elicits malignant progression of tumors to increased local invasion and distant metastasis. *Cancer Cell*, 15 (3); 220-231 (2009).
- [100] Gomez-Manzano C., Holash J., Fueyo J., et al. VEGF Trap induces antiglioma effect at different stages of disease. *Neuro-Oncology*, 10 (6); 940-945 (2008).
- [101] Carson-Walter E. B., Hampton J., Shue E., et al. Plasmalemmal vesicle associated protein-1 is a novel marker implicated in brain tumor angiogenesis. *Clinical cancer research*, 11; 7643-7650 (2005).

- [102] Beaty R. M., Edwards J. B., Boon K., et al. PLXDC1 (TEM7) is identified in a genome-wide expression screen of glioblastoma endothelium. *Journal of neuro-oncology* 81; 241-248, (2007).
- [103] Ricci-Vitiani L., Pallini R., Larocca L. M., et al. Mesenchymal differentiation of glioblastoma stem cells. *Cell Death and Differentiation*, 15; 1491-1498 (2008).
- [104] Bhat K. P., Balasubramaniyan V., Vaillant B., et al. Mesenchymal differentiation mediated by NF- $\kappa$ B promotes radiation resistance in glioblastoma. *Cancer Cell*, 24; 331-346 (2013).
- [105] Lester R. D., Jo M, Montel V., et al. uPAR induces epithelial-mesenchymal transition in hypoxic breast cancer cells. *The Journal of Cell Biology*, 178 (3); 425-436 (2007).
- [106] Wong H. K., Fatimy R. E., Onodera C., et al. The Cancer Genome Atlas analysis predicts microRNA for targeting cancer growth and vascularization in glioblastoma. *Molecular Therapeutics*, 23 (7); 1234-1247 (2015).
- [107] Hu B., Wang Q., AlanWang Y., et al. Epigenetic activation of WNT5A drives glioblastoma stem cell differentiation and invasive growth. *Cell*, 167; 1281-1295 (2016).
- [108] Cheng, C.W., Yeh, J.C., Fan, T.P., et al. Wnt5a-mediated non-canonical Wnt signalling regulates human endothelial cell proliferation and migration. *Biochemical and Biophysical Research Communications*, 365; 285-290 (2008).
- [109] Masckauchan T. N., Agalliu D., Vorontchikhina M., et al. Wnt5a signaling induces proliferation and survival of endothelial cells in vitro and expression of MMP-1 and Tie-2. *Molecular Biology of the Cell*, 17; 5163-5172 (2006).
- [110] Yang D.H., Yoon J.Y., Lee S.H., et al. Wnt5a is required for endothelial differentiation of embryonic stem cells and vascularization via pathways involving both Wnt/ $\beta$ -catenin and protein kinase Ca. *Circulation Research*, 104; 372-379 (2009).
- [111] Lian X., Bao X., Al-Ahmad A., et al. Efficient differentiation of human pluripotent stem cells to endothelial progenitors via small-

molecule activation of WNT signaling. *Stem Cell Reports*, 3; 804-816 (2014).

[112] Field K. M., Jordan J. T., Wen P. Y., et al. Bevacizumab and glioblastoma: scientific review, newly reported updates, and ongoing controversies. *Cancer*, 121 (7); 997-1007 (2015).

[113] Feng Q., Zhang C., Lum D., et al. A class of extracellular vesicles from breast cancer cells activates VEGF receptors and tumour angiogenesis. *Nature Communications*, 8; 14450 (2017).

[114] Lv L. H., Wan Y. L., Lin Y., et al. Anticancer drugs cause release of exosomes with heat shock proteins from human hepatocellular carcinoma cells that elicit effective natural killer cell antitumor responses in vitro. *The Journal of Biological Chemistry*, 287; 15874-15885 (2012).

[115] Baulch J. E., Geidzinski E., Tran K. K., et al. Irradiation of primary human gliomas triggers dynamic and aggressive survival responses involving microvesicle signaling. *Environmental and Molecular Mutagenesis*, 57; 405-415 (2016).

[116] Ricci-Vitiani L., Pedini F., Mollinari C., et al. Absence of caspase 8 and high expression of PED protect primitive neural cells from cell death. *The Journal of Experimental Medicine*, 200; 1257-1266 (2004).

[117] Chou C. H., Chang N. W., Shrestha S., et al. miRTarBase 2016: updates to the experimentally validated miRNA-target interactions database. *Nucleic acids research*, 44; 239-247 (2016).

[118] Subramanian A., Tamayo P., Mootha V. K., et al. Gene set enrichment analysis: a knowledge-based approach for interpreting genome-wide expression profiles. *Proceedings of the National Academy of Science U.S.A.*, 102; 15545-15550 (2005).

[119] Signore M., Buccarelli M., Pilozzi E., et al. UCN-01 enhances cytotoxicity of irinotecan in colorectal cancer stem-like cells by impairing DNA damage response. *Oncotarget*, 7 (28); 44113-44128 (2016).

---

- [120] Tate C. M., Pallini R., Ricci-Vitiani L., et al. A BMP7 variant inhibits the tumorigenic potential of glioblastoma stem-like cells. *Cell Death and Differentiation*, 19; 1644-1654 (2012).
- [121] Gentleman R. C., Carey V. J., Bates D. M., et al. Bioconductor: open software development for computational biology and bioinformatics. *Genome Biology*, 5 (10): R80 (2004).
- [122] Ritchie M. E., Phipson B., Wu D., et al. limma powers differential expression analyses for RNA-sequencing and microarray studies. *Nucleic acids research*, 43; e47 (2015).